

1
2
3
4
5
6
7
8
9
10
11
12
13
14
15
16
17
18
19
20
21
22
23
24
25
26
27
28
29
30
31
32
33
34
35
36
37
38
39
40

Geodynamic implications of ophiolitic chromitites in the La Cabaña ultramafic bodies, Central Chile

José María González-Jiménez

*Departamento de Geología and Andean Geothermal Center of Excellence (CEGA),
Facultad de Ciencias Físicas y Matemáticas, Universidad de Chile, Santiago, Chile*

E-mail: jmgonzj@ing.uchile.cl

Fernando Barra

*Departamento de Geología and Andean Geothermal Center of Excellence (CEGA),
Facultad de Ciencias Físicas y Matemáticas, Universidad de Chile, Santiago, Chile*

Richard J. Walker

Department of Geology, University of Maryland, College Park, MD 20742, USA

Martin Reich

*Departamento de Geología and Andean Geothermal Center of Excellence (CEGA),
Facultad de Ciencias Físicas y Matemáticas, Universidad de Chile, Santiago, Chile*

Fernando Gervilla

*Departamento de Mineralogía y Petrología and Instituto Andaluz de Ciencias de la
Tierra (Universidad de Granada-CSIC), Fuentenueva s/n, Granada, Spain.*

41 **Abstract**

42 Chromitites (> 80% volume chromite) hosted in two ultramafic bodies (Lavaderos
43 and Centinela Bajo) from the Palaeozoic metamorphic basement of the Chilean
44 Coastal Cordillera were studied in terms of their chromite composition, platinum-
45 group element (PGE) abundances and Re-Os isotopic systematics. Primary chromite
46 ($Cr\#=0.64-0.66$; $Mg\#=48.71-51.81$) is only preserved in some massive chromitites
47 from the Centinela Bajo ultramafic body. This chemical fingerprint is similar to other
48 high-Cr chromitites from ophiolite complexes, suggesting that they crystallised from
49 arc-type melt similar to high-Mg island-arc tholeiites (IAT) and boninites in supra-
50 subduction mantle. The chromitites display enrichment in IPGE (Os, Ir, Ru) over
51 PPGE (Rh, Pt, Pd), with PGE concentrations between 180 and 347 ppb, as is typical
52 of chromitites hosted in the mantle of supra-subduction zone (SSZ) ophiolites. Laurite
53 (RuS_2)-erlichmanite (OsS_2) phases are the most abundant inclusions of platinum-
54 group minerals (PGM) in chromite, indicating crystallisation from S-undersaturated
55 melts in the sub-arc mantle. The metamorphism associated with the emplacement of
56 the ultramafic bodies in the La Cabaña has been determined to be ca. 300 Ma, based
57 on K-Ar dating of fuchsite. Initial $^{187}Os/^{188}Os$ ratios for four chromitite samples,
58 calculated for this age, range from 0.1248 to 0.1271. These isotopic compositions are
59 well within the range of chromitites hosted in the mantle section of other
60 Phanerozoic ophiolites. Collectively, these mineralogical and geochemical features
61 are interpreted in terms of chromite crystallisation in dunite channels beneath a
62 spreading center that opened a marginal basin above a supra-subduction zone. This
63 implies that chromitite-bearing serpentinites in the metamorphic basement of the
64 Coastal Cordillera are of oceanic-mantle origin and not oceanic crust as previously
65 suggested. We suggest that old subcontinental mantle underlying the hypothetical
66 Chilenia micro-continent was unroofed and later altered during the opening of the
67 marginal basin. This defined the compositional and structural framework in which the
68 protoliths of the meta-igneous and meta-sedimentary rocks of the Eastern and
69 Western Series of the Chilean Coastal Cordillera basement were formed.

70

71 **Keywords:** Chromite; ophiolite; marginal basin; Chile; Chilenia

72

73

74

75 1. Introduction

76 The Palaeozoic metamorphic basement of the Chilean south-central Coastal
77 Cordillera contains scattered small bodies of serpentinised ultramafic rocks associated
78 with a heterogeneous assemblage of meta-sedimentary and meta-volcanic rocks
79 (Aguirre *et al.* 1972; Hervé 1974, 1977; Godoy and Kato 1990; Willner *et al.* 2005;
80 Glodny *et al.* 2008). These ultramafic bodies and their host rocks have been suggested
81 to be slices of fossil oceanic lithosphere, which were accreted to the Pacific margin of
82 Gondwana (Hervé *et al.* 1981; Forshythe 1982; Glodny *et al.* 2005; Willner *et al.*
83 2005). The origin of the ultramafic rocks has been the subject of many studies and
84 remains a hotly debated topic with two main hypotheses. An initial survey by Barra *et*
85 *al.* (1998) of chromitite samples collected from streams draining the largest ultramafic
86 bodies in the area of La Cabaña, about 60 km west of the city of Temuco (Fig. 1),
87 revealed that these chromitites have an island arc geochemical signature.
88 Additionally, Höfer *et al.* (2001) integrated the petrology and ages of deposition and
89 metamorphism of the meta-sedimentary rocks with the mechanism of emplacement of
90 the meta-volcanic and ultramafic rocks from La Cabaña, concluding that these rocks
91 represent portions of oceanic lithosphere formed in a marginal basin developed
92 behind an island arc, sited on the Paleo-Pacific margin of Gondwana. In contrast,
93 Glodny *et al.* (2005) and Willner *et al.* (2005), based on studies of the northern part of
94 the Coastal Cordillera (34°-36° S), have suggested that these are oceanic crustal rocks
95 that were incorporated into the Coastal Cordillera by basal accretion.

96 These observations and contrasting models raise questions about the true origin of
97 the chromitites and their host ultramafic rocks at La Cabaña, as well as their
98 relationships to the surrounding meta-sedimentary and meta-volcanic rocks. In an
99 attempt to bridge this gap we examined the geochemistry of platinum-group elements
100 (PGE), Re-Os isotopes and *in situ* chemical analyses of chromite in chromitites from
101 the La Cabaña ultramafic bodies. Our study contributes important data to the ongoing
102 debate regarding interpretations of the origin and evolution of the metamorphic
103 basement of the Chilean Coastal Cordillera, and provides new insights into the
104 evolution of the Palaeozoic eastern margin of the Gondwana supercontinent.

105

106 **Geology of the chromitites**

107 *Geological overview of the metamorphic basement of central Chile*

108 The La Cabaña ultramafic bodies (after [Vergara 1970](#)) are situated near the town
109 of Carahue in central Chile, approximately 60 km west of Temuco ([Fig. 1](#)).
110 Geologically, they are part of the Palaeozoic metamorphic basement of the Chilean
111 Coastal Cordillera, a paired metamorphic belt of Palaeozoic age that extends for more
112 than 1,000 km along the south-central part of the Pacific coast of Chile. The
113 westernmost unit of this metamorphic belt is known as the Western Series, whereas
114 the easternmost belt is termed the Eastern Series. The rocks of these two units record
115 distinct metamorphic grades: high-pressure/low-temperature (HP-LT) in the Western
116 Series and low-pressure/high-temperature (LP-HT) in the Eastern Series (e.g., [Aguirre](#)
117 [et al. 1972](#); [Godoy and Kato 1990](#); [Willner et al. 2005](#)). The boundary between the
118 two units is the sinistral NW-SE-striking Lanalhue Fault Zone ([Glodny et al. 2008](#)) in
119 the south, whereas it is marked by a late reverse structure, the Pichilemu-Vichuquén
120 Fault in the north ([Willner et al. 2005](#)).

121 The Western Series comprises meta-greywackes containing lenses of greenschists
122 and blueschists and associated Fe, Mn-rich meta-sediments, meta-cherts and bodies of
123 mafic-ultramafic rocks (upper mantle dunite, cumulate dunite-pyroxenites and
124 gabbros), with some of them deformed and metamorphosed together with the
125 surrounding host rocks ([Aguirre et al. 1972](#); [Hervé 1977](#); [Frutos and Alfaro 1987](#);
126 [Barra et al. 1998](#); [Höfer et al. 2001](#)). [Höfer et al. \(2001\)](#) suggested an island arc
127 position for the chromitites, which they interpreted as having a back-arc setting on
128 the basis of data from the neighbouring rocks. Although limited isotopic data exist for
129 the metamorphic host rocks (e.g., [Hervé et al. 2013](#)), no isotopic data have been
130 obtained so far for the mafic-ultramafic rocks.

131 The Eastern Series consists of alternating psammites and metapelites characterised
132 by very low grades of metamorphism; these rocks are weakly deformed and mostly
133 preserve the original bedding, except in the easternmost part of the belt where higher
134 metamorphic grade has obliterated the primary fabric of the rocks ([Willner et al.](#)
135 [2000](#); [Hervé et al. 2013](#)).

136 The rocks of the Coastal Cordillera have been interpreted as either an accretionary
137 complex (Hervé *et al.* 1981; Glodny *et al.* 2005, 2008; Willner 2005; Willner *et al.*
138 2005), or a backarc basin (Frutos and Alfaro 1987; Rabbia *et al.* 1994; Hufmann and
139 Massonne 2000; Höfer *et al.* 2001) formed during the Late Carboniferous.

140 *The La Cabaña Ultramafic Bodies*

141 The La Cabaña ultramafic bodies consist of two small outcrops (Barra *et al.* 1998):
142 the Centinela Alto (or Lavanderos) to the east and Centinela Bajo to the west (Fig. 2).

143 Lavanderos is a lens-like ultramafic body 200 × 35 m in size, trending NE-SW. It
144 is hosted in Palaeozoic mica-schists enclosing meta-volcanic rocks (Fig. 2; Vergara
145 1970; Alfaro 1980; Höfer *et al.* 2001). The body largely consists of antigorite, with
146 accessory clinocllore and chromite mostly transformed to Fe²⁺-rich porous chromite
147 (Alfaro 1980; Barra *et al.* 1998). Talc locally replaces both antigorite and chlorite.
148 The antigorite shows a penetrative mylonitic foliation towards the boundaries of the
149 body, which was most likely produced during its fault-controlled emplacement (Barra
150 *et al.* 1998), or during greenschist-facies metamorphism (Höfer *et al.* 2001).

151 Centinela Bajo is a larger oblate body of 6 × 3 km in size that protrudes into the
152 mica-schists. The rocks are dunites made up of coarse-grained porphyroclastic olivine
153 (1-2 mm) replaced by pseudomorphic (mesh texture) lizardite, with minor amounts of
154 primary pyroxenes. The degree of alteration of the primary silicates may vary from 20
155 to 80% volume of the rock. The secondary silicates are accompanied by secondary
156 chlorite and amphibole, and a late generation of chrysotile and carbonate veins cross-
157 cutting all of the described minerals. Höfer *et al.* (2001) described an outcrop of meta-
158 gabbros in contact with dunites in the northern part of the ultramafic body. However,
159 in our field studies we did not find a continuous section from the mantle dunite to
160 gabbros, owing to poor exposure in the rainforest. Despite the poor exposure Höfer *et*
161 *al.* (2001) reported that the gabbros show clear evidence of metamorphism
162 (uralitisation of clinopyroxene, secondary chlorite and minor zoisite and titanite),
163 unlike the peridotites supposedly in contact with them. Detailed structural mapping
164 reveals that shear zones filled by mylonitised serpentinite surround and isolate blocks
165 of undeformed serpentinitised dunite; in the latter, mantle foliation (defined by trains of
166 Cr-spinel in the porphyroclastic rocks) and random distributions of Cr-spinel grains

167 are obliterated by the late mylonitic foliation near the contacts with the shear zones.
168 The foliations in the serpentinite rocks have a strike and dip identical to the foliation
169 of the host schists (Höfer *et al.* 2001; Fig. 2).

170 *Chromitites*

171 Chromitites have been reported in both ultramafic bodies at La Cabaña (Fig. 2 and
172 3; Barra *et al.* 1998; Höfer *et al.* 2001), although chromitites have only been observed
173 *in situ* in Lavaderos (Fig. 3a-e). The Lavaderos chromitites are lenses and veins of
174 a few centimetres thick of massive chromite (>80% chromite grains) hosted in heavily
175 serpentinitised dunite (Fig. 3a-c). The contact between the massive chromitite and the
176 host rock is sharp (Fig. 3c) but can locally grade to disseminated chromite ore through
177 a zone of schlieren chromite (Fig. 3a-b). Frequently, late veins of chrysotile transgress
178 the chromitite veins, disrupting their continuity (Fig. 3b-c). The metamorphic
179 alteration that affected the rocks of the body has also completely transformed the
180 magmatic chromite to secondary Fe²⁺-rich porous chromite (Fig 4a; Barra *et al.* in
181 press).

182 At Centinela Bajo, the poor exposure in the forest does not allow for direct
183 observation of the chromitite bodies. We only identified a few boulders of massive
184 chromitite on the slopes of the vegetation-covered hills (Fig. 2 and 3d-e). The features
185 of these boulders, such as the massive texture of the ore, their irregular to angular
186 shape and relatively large size, and their distribution along the drainage network
187 suggest the presence of hidden large chromitite bodies (Fig. 2; Höfer *et al.* 2001). The
188 studied chromitite blocks consist of >80% former euhedral chromite grains, which
189 are fractured and complexly zoned (Fig. 4b). The zoning consists of
190 crystallographically-ordered rims (or patches) of Fe²⁺-rich chromite (Barra *et al.* in
191 press) surrounding the unaltered (magmatic) cores. In the altered rims there are
192 abundant inclusions of Cr-clinochlore, which may also fill one of the generations of
193 fractures cutting the chromite grains. Cr-clinochlore is also the main constituent of the
194 interstitial matrix between chromite grains (Barra *et al.* in press).

195 **Methods**

196 The compositions of major and minor elements in primary igneous cores of
197 chromian spinels were obtained using a SX-100 CAMECA electron microprobe
198 analyser (EMPA) at the Centro de Instrumentación Científica of the University of
199 Granada (Spain), using the procedures described by [Gervilla *et al.* \(2012\)](#). In the
200 former, calibration for chromite was performed using natural and synthetic standards:
201 MgO for Mg, Fe₂O₃ for Fe, Al₂O₃ for Al, Cr₂O₃ for Cr, SiO₂ for Si, TiO₂ for Ti,
202 MnTiO₃ for Mn, NiO₂ for Ni and Pb₅(VO₄)₃Cl for V.

203 Six chromitite samples were analysed for bulk platinum-group elements (PGE)
204 abundances. The analyses were performed by Actlabs, Canada using nickel sulfide
205 fire assay and instrumental neutron activation analysis (INAA) technique. Detection
206 limits were 5 ppb for Ru and Pt, 2 ppb for Os and Pd, 0.2 ppb for Rh, and 0.1 for Ir.

207 Whole-rock Re-Os isotopic analyses were performed on mineral separates of
208 chromite from four selected chromitite samples. Chromite grains were analysed at the
209 Isotope Geochemistry Laboratory, University of Maryland, USA, following the
210 procedure described by [Walker *et al.* \(2002a\)](#). Briefly, about 0.5g of finely-ground
211 chromite was introduced into a Pyrex™ Carius tube with a 2:1 mixture of
212 concentrated nitric and hydrochloric acids, and appropriate amounts of a mixed Re-Os
213 spike. The tube was then sealed and heated at 270 °C for >24 hours. Upon opening
214 the tube, Os was separated by solvent extraction techniques ([Cohen and Waters 1996](#))
215 and Re by standard column-chemistry procedure ([Morgan and Walker 1989](#)).
216 Osmium was further purified by microdistillation ([Birck *et al.* 1997](#)). Osmium
217 isotopic ratios were determined using the UMd *VG Sector 54* thermal ionisation mass-
218 spectrometry (TIMS) using Faraday cups, whereas Re abundances were analysed
219 using a Cetac Aridus nebuliser coupled to a Nu Plasma multi-collector inductively-
220 coupled plasma-mass spectrometer (MC-ICP-MS). External precision for ¹⁸⁷Os/¹⁸⁸Os,
221 and Os and Re concentrations for the quantities measured was better than 0.1%, 0.2%
222 and 2% respectively. Procedure blanks averaged 0.8 picograms for Os and 1.2
223 picograms for Re. Blank corrections for Os were negligible (<0.1%). Blank
224 corrections for Re comprised as much as 1% for some samples. Initial ¹⁸⁷Os/¹⁸⁸Os
225 ratios are calculated as per [Shirey and Walker \(1998\)](#).

226

227 **Results**

228 *Chemistry of primary chromite*

229 As the La Cabaña chromitites are variably altered, interpretations of their
230 petrogenesis in terms of primary magmatic processes in the mantle require the
231 analysis of the unaltered cores of chromite grains. Primary cores were only preserved
232 in the massive chromitite of Centinela Bajo (Fig 4b and 5a-d; Barra *et al.* 1998). The
233 assumption of an igneous origin for these cores is supported by EMPA analyses
234 showing that they contain very low Fe₂O₃ (<2.60 wt.%; *i.e.*, [Fe³⁺# =
235 Fe³⁺/(Fe³⁺+Al³⁺+Cr³⁺)] <0.03), high MgO (>12.09 wt.%), and low TiO₂ (<0.23 wt.%),
236 values that are typical for primary chromite from mantle-hosted ophiolitic chromitites
237 (Fig. 5a-b; Table 1).

238 The primary chromite of the Centinela Bajo chromitites is highly homogeneous in
239 terms of Cr# [Cr/(Cr+Al) atomic ratio] and Mg# [Mg/(Mg+Fe²⁺) atomic ratio] (Fig.
240 5c). Thus, the Cr# values range between 0.64 and 0.66, which correspond to 48.71-
241 51.81 wt% Cr₂O₃ and 17.33-18.52 wt.% Al₂O₃, whereas the Mg# varies from 0.58 to
242 0.67. These Cr# and Mg# values overlap with the compositional field of high-Cr
243 podiform ophiolitic chromitite (Fig. 5a-c; Leblanc and Nicolas 1992). The contents of
244 MnO, V₂O₃ and ZnO are lower than 0.48 wt.%, 0.29 wt.% and 0.20 wt.%,
245 respectively.

246 *Platinum-group elements (PGE)*

247 The La Cabaña chromitites have relatively low PGE concentrations, with total
248 PGE contents ranging from 180 to 347 ppb for each of the samples (Table 2), with
249 slightly higher concentrations in samples from Centinela Bajo (294-347 ppb; mean
250 320 ppb) relative to those from Lavaderos (180-235; mean 213 ppb). Figure 6 shows
251 the chondrite-normalised distribution pattern of the La Cabaña chromitites compared
252 with chromitites hosted in the mantle sections of other ophiolites, and from other
253 geodynamic settings. The general compositional trend of the La Cabaña chromitites
254 fits very well with the distribution of the PGEs shown by other Type I chromitites
255 (González-Jiménez *et al.* 2014a) that are hosted in the mantle sequence of ophiolite

256 complexes and show an enrichment in the IPGE (Os, Ir and Ru =305-346.9 ppb)
257 relative to the PPGE (Rh, Pt and Pd=13.9-42.9 ppb).

258 The La Cabaña chromitites exhibit steep positive patterns from Os to Ru (with
259 positive Ir anomalies relative to Os and Ru in the samples CAB-7B and PODOB),
260 followed by steep negative slopes from Rh to Pd (with Pd positive anomalies in the
261 samples CAB-7B, LAC-2). This distribution of the PGEs in the La Cabaña
262 chromitites also overlaps the fields of other Latin American chromitites hosted in the
263 mantle sections of supra-subduction zone (SSZ) ophiolites (Fig. 6a-c), such as the
264 “unmetamorphosed” high-Cr chromitites in Sagua de Tánamo, eastern Cuba
265 (González-Jiménez *et al.* 2011), in Santa Elena in the Dominican Republic (high-Cr
266 and high-Al; Fig. 6b; Zaccarini *et al.* 2011), and in the “metamorphosed” high-Al
267 chromitites of Tehuiztingo, SW Mexico (Proenza *et al.* 2004). In contrast, the La
268 Cabaña chromitites have lesser amounts of IPGE and a less pronounced negative
269 segment from IPGE to PPGE than the chromitites (high-Cr) of the Vizcaino
270 Peninsula, Mexico (Fig. 6b; Vatin-Perignon *et al.* 2000). These chromitites are
271 interpreted to have crystallised in equilibrium with melts of boninitic affinity,
272 generated by hydrous melting in suprasubduction environments. Finally, the La
273 Cabaña chromitites are significantly different from the high-Al chromitites of the
274 Pampean Ranges, Argentina, in which metamorphism has disturbed the original
275 distribution of PGEs (Fig. 6c; Proenza *et al.* 2008).

276 The abundances of IPGE in the La Cabaña chromitites were controlled by
277 abundant small inclusions (<25 µm) of Os-Ir-Ru alloys, laurite (RuS₂)-erlichmanite
278 (OsS₂), irarsite (IrAsS), and minor omeiite (OsAs₂), and Ru-Ni alloys (Galdames *et*
279 *al.* 2011). The PPGE-rich assemblage mainly includes Rh-rich minerals, such as
280 hollingworthite (RhAsS), and an unidentified antimonide (Rh-Cu-Sb). Laurite-
281 erlichmanite is found as inclusions in the cores of chromite grains but is more
282 frequently replaced by Os-Ir-Ru alloys in pores of Fe²⁺-rich chromite, suggesting its
283 desulfurisation under reducing conditions. This process could be also responsible for
284 the formation of Ru-Ni alloys after breakdown of Ru-bearing Ni-rich sulfides. In
285 contrast, irarsite, omeiite and the unnamed Rh-Cu antimonide are most likely
286 associated with oxidising fluids, which supplied As and Sb to the system, and
287 redistributed the PGE. Abundant secondary inclusions of Ni-rich S-poor sulfides

288 (heazlewoodite and gersdorffite) and Ni-arsenides accompany these PGM in the
289 alteration rims of chromite.

290 *Whole-rock Re-Os isotopes*

291 Total Re contents in La Cabaña chromitites are very low (<0.35 ppb), with the
292 exception of sample CEN-07, which shows a slightly higher Re content (2.2 ppb).
293 Osmium concentrations vary from 38 to 202 ppb (Table 3). Measured $^{187}\text{Os}/^{188}\text{Os}$
294 ratios of chromite separates from three chromitite blocks of Centinela Bajo vary from
295 0.1252 to 0.1271, and a chromite separate from one chromitite pod from Lavanderos
296 has a ratio of 0.1268 (Table 3). The $^{187}\text{Os}/^{188}\text{Os}$ for all four chromitite samples
297 averages of 0.12652 ± 0.0008 (2σ). Estimates for the present $^{187}\text{Os}/^{188}\text{Os}$ ratio of the
298 bulk oceanic mantle range from a low of ~ 0.125 , based on the average of abyssal
299 peridotites (e.g., Snow and Reisberg 1995; Liu *et al.* 2009), to a high of ~ 0.128 , based
300 on averages for chromitites and peridotites of Phanerozoic ophiolites extrapolated to
301 the present (e.g., Walker *et al.* 2002b). Thus, ratios for all of our chromitite samples
302 fall well within the range of estimates for the modern oceanic mantle.

303 Initial $^{187}\text{Os}/^{188}\text{Os}$ ratios have been calculated for 300 Ma, which is the estimated
304 age of emplacement of the peridotites onto the continental crust inferred from the age
305 of metamorphism of the meta-sedimentary rocks hosting the peridotites (Höfer *et al.*
306 2001; Willner *et al.* 2005). These ratios are almost identical to the measured ratios
307 because of the very low Re/Os ratios of the chromitites. At La Cabaña, the initial
308 $^{187}\text{Os}/^{188}\text{Os}$ ratios span from 0.1248 to 0.1271, with an average of 0.1264 ± 0.0011
309 (2σ) (Fig. 7). Although the total number of samples analysed for Os isotopes is too
310 small to be statistically robust, there appear to be no major differences in Os isotopic
311 compositions between chromitites of Centinela Bajo and Lavanderos.

312 **Discussion**

313 *Parental melts of the chromitites*

314 The composition of primary magmatic cores of chromite from Centinela Bajo
315 chromitites with high Cr, and low Fe_2O_3 and TiO_2 contents is typical of chromite from
316 chromitites hosted in the upper mantle sequence of ophiolite complexes (Fig. 5a-b). In
317 the diagram Al_2O_3 versus TiO_2 defined by Kamenetsky *et al.* (2001) for chromites

318 hosted in lavas of different geotectonic settings (Fig. 5d), some of these cores fall
 319 within the field of MORB and within the field of spinels with high Ti from basalts of
 320 modern back-arc basins; another set of data with lower TiO₂ plots out of these fields.
 321 This scattering in the plot is a common feature of many mantle-hosted chromitites
 322 worldwide (e.g., Pagé and Barnes 2009; Zaccarini *et al.* 2011; Escayola *et al.* 2011),
 323 which may reflect the increase of TiO₂ produced in melts crystallising chromitite as
 324 they migrate through the SSZ mantle while reacting with peridotite wall-rock
 325 (Graham *et al.* 1996; Zaccarini *et al.* 2011; González-Jiménez *et al.* 2011, 2014b).

326 Experimental and empirical studies show that the contents of Al₂O₃, TiO₂, FeO and
 327 MgO in chromite reflect those of the melt from which the chromite has crystallised
 328 (Maurel and Maurel 1982; Wasylenki *et al.* 2003; Kamenetsky *et al.* 2001; Rollinson
 329 2008; Pagé and Barnes 2009). Considering that our chromites are high-Cr and low-Ti
 330 (Fig. 5a-d), similar to chromite from low-Ti high-Cr arc-lavas of Kamenetsky *et al.*
 331 (2001), we have estimated the Al₂O₃ and TiO₂ contents of the melt(s) in equilibrium
 332 with our chromite using the revised equations defined by Zaccarini *et al.* (2011) for
 333 those chromites (eqs. 1 and 2):

$$334 \ln [\text{wt}\% \text{Al}_2\text{O}_3 (\text{melt})] = 5.2253 \times \ln [\text{Al}_2\text{O}_3 (\text{spinel})] - 1.1232 \quad (R^2=0.9723) \quad (\text{eq. 1})$$

$$335 \ln [\text{wt}\% \text{TiO}_2 (\text{melt})] = 1.0897 \ln [\text{wt}\% \text{TiO}_2 (\text{spinel})] + 0.0892 \quad (\text{eq. 2})$$

336 The FeO/MgO ratios of the melts in equilibrium with Centinela Bajo chromites
 337 were estimated using the following empirical expression (Maurel and Maurel 1982;
 338 equation 3):

$$339 \ln(\text{FeO/MgO})_{\text{spinel}} = 0.47 - 1.07\text{Al}\#_{\text{spinel}} + 0.64\text{Fe}^{3+}\#_{\text{spinel}} + \ln(\text{FeO/MgO})_{\text{melt}} \quad (\text{eq. 3})$$

340 where FeO and MgO in wt%, Al# = Al/(Cr+Al+Fe³⁺) and Fe³⁺# = Fe³⁺/(Cr+Al+Fe³⁺).

341 These calculations suggest that the melts that have precipitated the chromite of the
 342 Centinela Bajo chromitites contained from 13.7 to 14.2 wt% Al₂O₃, and from 0.22 to
 343 0.34 wt% TiO₂, with the FeO/MgO ratio varying between 0.8 and 1.2. The Al₂O₃
 344 contents of the parental melt in equilibrium with the igneous chromite of the
 345 Centinela Bajo are similar to the melts that precipitated the high-Cr chromites in
 346 boninite lavas at Bonin Island in Japan (10.6-14.4 wt.% Al₂O₃; Hicky and Frey 1982;

347 Crawford *et al.* 1989), but also overlap those of high-Mg island-arc tholeiites (IAT)
348 (11.4-16.4 wt.% Al₂O₃; Augé 1987).

349 Similar arc-type melts, but with lower Al₂O₃, TiO₂ and FeO/MgO ratios, have been
350 suggested to be responsible for the formation of high-Cr chromitites in the mantle
351 section of many SSZ ophiolites. Examples include Kempirsai in Kazakhstan (Melcher
352 *et al.* 1997), Oman (Rollinson 2008), Muğla in Turkey (Uysal *et al.* 2009), Rutland
353 Island in the Bay of Bengal (Ghosh *et al.* 2009), Santa Elena in Costa Rica (Zaccarini
354 *et al.* 2011), and Mayarí-Cristal, in eastern Cuba (Proenza *et al.* 1999; González-
355 Jiménez *et al.* 2011). These chromitites were interpreted to have crystallised near the
356 Moho Transition Zone (MTZ) of oceanic lithosphere overlying a subduction zone in
357 either a fore-arc or back-arc basin.

358 On the other hand, the La Cabaña chromitites show the typical chondrite-
359 normalised PGE patterns of ophiolitic chromitites characterised by the enrichment in
360 IPGE (i.e., Os, Ir and Ru), which differ significant from chromitites found in layered
361 mafic intrusions and Ural/Alaskan complexes (Fig. 6a). The inclusions of primary Os-
362 rich PGM like laurite, as a mineralogical expression of the abundances of IPGEs,
363 indicate the sulfur-undersaturated nature of the melts that crystallised the chromitites
364 (Garuti *et al.* 1999; Brenan and Andrews 2001; Andrews and Brenan 2002; Bockrath
365 *et al.* 2004). Basaltic melts with low enough fS_2 to precipitate Os-rich PGM are
366 produced during the partial melting of depleted peridotites (Jugo 2009), or
367 secondarily by the reaction of IAT melts with mantle peridotite at increasing
368 melt/rock ratio during the formation of chromitites, in SSZ mantle (Zhou *et al.* 1998;
369 Büch *et al.* 2002; Shi *et al.* 2007; Marchesi *et al.* 2011).

370 *Tectonic setting of the La Cabaña ultramafic bodies*

371 According to Prichard *et al.* (2008), chromitites with appreciable amounts (~100
372 ppb) of total PGEs are precipitated only from melts that have been extracted after
373 ≥20% partial melting of mantle sources. The fact that at La Cabaña the average PGE
374 content of chromitites is around 250 ppb suggests that the melts were derived from a
375 mantle source that had experienced degrees of partial melting above 20%. The
376 primary olivine preserved in the dunites at Centinela Bajo have Mg# = 0.90-0.92 and
377 NiO contents (0.16-0.45 wt.%), similar to the olivine in the ultra-depleted peridotites

378 of the mantle sections of ophiolites of Eastern Cuba (Fig. 8). This leads us to suggest
379 that the dunites hosting the chromitites at Centinela Bajo are residues resulting from
380 high degrees of partial melting.

381 In the ophiolite environment, peridotites that have undergone multiple episodes of
382 melt extraction until nearly barren in their major- and minor-elements signatures are
383 common in the mantle beneath arcs developed above supra-subduction zones (e.g.,
384 [Ohara *et al.* 2002](#); [Marchesi *et al.* 2006](#); [Ishimaru *et al.* 2007](#)). In these settings,
385 dehydration of the subducting slab may release a large volume of volatiles
386 contributing to a decrease in the melting temperature, thus favouring the release of
387 PGEs from their host peridotitic mantle at lower degrees of partial melting than
388 relatively fertile, “dry” and less oxidised settings such as MOR ([Jugo 2009](#)).
389 Chromitites that have crystallised in a MOR setting are significantly more depleted in
390 PGEs than those from the La Cabaña (frequently <100 ppb; [Leblanc and Nicolas
391 1992](#); [Zhou *et al.* 1996, 1998](#); [Proenza *et al.* 1999](#); [Ahmed and Arai 2002](#); [Prichard *et
392 al.* 2008](#); [Uysal *et al.* 2009](#); [González-Jiménez *et al.* 2014a](#)).

393 The similar geochemistry of the studied chromitites to “mantle hosted” chromitites
394 from SSZ ophiolites provide the first evidence that the La Cabaña ultramafic bodies
395 are portions of an oceanic mantle overlying a supra-subduction zone. The formation
396 of chromitites in the suprasubduction zone environment is commonly associated with
397 the crystallisation of basaltic melts at their site of extraction during the opening of
398 marginal basins in either fore-arc or back-arc basins ([Roberts 1998](#); [Leblanc and
399 Nicolas 1992](#); [Malpas 1997](#); [Melcher *et al.* 1997](#); [Proenza *et al.* 1999](#); [Rollinson,
400 2005, 2008](#); [Gervilla *et al.* 2005](#); [Robinson and Adetunji 2013](#); [González-Jiménez *et
401 al.* 2014b](#)). This is consistent with the fact that the widespread meta-volcanic rocks
402 and metabasites in the Western Series show E-MORB signatures ([Rabbia *et al.* 1994](#);
403 [Hufmann and Massone 2000](#)), suggesting that these rocks crystallised from basaltic
404 melts derived from an upwelling mantle beneath a spreading center. During the
405 formation and evolution of the marginal basin above a supra-subduction zone, the
406 extraction of melts from the mantle takes place preferentially through dunite conduits
407 sited beneath the axis of the spreading ridge. Numerical modelling ([Braun and
408 Kelemen 2002](#)) shows that in these settings the dunite conduits form an
409 interconnected network of channels filled with basaltic melts that might be extracted

410 from different mantle sources. Where two or more melt-filled conduits intersect,
411 batches of melt with different degrees of fractionation (i.e., different αSiO_2) may mix
412 to produce hybrid melts saturated with chromite, and thus, are capable of crystallising
413 sizeable chromitite bodies (González-Jiménez *et al.* 2014b).

414 Under the proposed scenario, the upwelling arc-type melts might become saturated
415 in chromite, precipitating chromitites prior to their emplacement at crustal levels as
416 mafic rocks or extruded lavas. A similar interpretation has been proposed for other
417 ophiolites (Leblanc 1986; Graham *et al.* 1996; González-Jiménez *et al.* 2011), and
418 demonstrated by analysis of minor- and trace-element in chromite from a suite of
419 mantle and crustal rocks of Oman (Dare *et al.* 2009) and Thetford Mines in Canada
420 (Pagé and Barnes 2009). Thus, our observations and data provide significant evidence
421 against previous interpretations that the metabasites and their associated ultramafic
422 rocks (i.e., serpentinites and peridotites) found in the metamorphic basement of the
423 Coastal Cordillera represent the segments of *the upper part of an oceanic crust*
424 (Willner 2005). In contrast, we propose that these rocks correspond to different
425 fragments of oceanic lithosphere (including mantle and overlying crust) that
426 originally formed in a marginal basin developed above a supra-subduction zone. Most
427 likely these portions of upper mantle were later incorporated into the continental crust
428 by basal accretion within the accretion prism represented by the metamorphic rocks of
429 the Coastal Cordillera.

430 *Interpretation of the Re-Os isotopic data*

431 As is typical of ophiolitic chromitites worldwide, the four La Cabaña
432 chromites are characterised by very low $^{187}\text{Re}/^{188}\text{Os}$ ratios, hence calculated initial
433 ratios are not very sensitive to age correction. Here, we have used the estimated age of
434 the host rocks metamorphism (ca. 300 Ma) to calculate the initial $^{187}\text{Os}/^{188}\text{Os}$ ratio.
435 However, it is reasonable to think that this is a minimum age because the chromitites
436 and their PGM and base-metal sulfide (BMS) inclusions could have formed several
437 million years before their emplacement onto the continental crust (e.g., González-
438 Jiménez *et al.* 2014a). Of note, the initial $^{187}\text{Os}/^{188}\text{Os}$ ratios of the La Cabaña
439 chromites fit well with the average evolution curve for chromitites of SSZ ophiolites
440 worldwide (Fig. 7; Walker *et al.* 2002b).

441 The initial $^{187}\text{Os}/^{188}\text{Os}$ ratios of La Cabaña chromites, however, vary little
442 compared with much larger variations noted for most other chromites from
443 Phanerozoic ophiolites (Fig. 7a). Büchl *et al.* (2004) also observed small variations of
444 Os in chromitite pods hosted in the mantle section of the Troodos ophiolite. In these
445 chromites the range of variation of $^{187}\text{Os}/^{188}\text{Os}$ ratios of the chromite separates
446 (0.1265-0.1301) is much lower than those of the associated peridotites (0.1235-
447 0.1546). This observation is in agreement with more recent data by O'Driscoll *et al.*
448 (2012) for the Shetland Ophiolite chromites, where whole rock $^{187}\text{Os}/^{188}\text{Os}$ for
449 discrete chromitite pods is remarkably homogenous, albeit with significant
450 heterogeneities observed in chromites from different localities. These authors
451 suggest that during the formation of the chromites under an open-system, potentially
452 with significant input of numerous melts with variable composition, the mixing
453 process involved in the formation of chromites tend to homogenize the Os
454 signatures. This is surprising, as the Os isotopic compositions are likely governed by
455 the presence of discrete inclusions of PGM and BMS formed from melt/fluids with
456 diverse magmatic and possibly post-magmatic contributions (Fig. 7; Malitch *et al.*
457 2003; Malitch 2004; Ahmed *et al.* 2006; Shi *et al.* 2007; Marchesi *et al.* 2011;
458 González-Jiménez *et al.* 2012a,b, 2013a, 2014a).

459 Additionally, recent studies of ophiolite chromitite have shown that they often
460 contain several populations of PGM and BMS, with different Os-isotope signatures at
461 the sub-grain scale (e.g., Marchesi *et al.* 2011; González-Jiménez *et al.* 2012a,b,
462 2013a, 2014a). The *in-situ* analysis, using LA-MC-ICPMS, of large numbers of
463 individual PGM and BMS from chromites and host peridotites in the Ojén massif in
464 Spain suggest that the formation of these chromites, which involved partial melting,
465 melt transport/pooling and melt–rock reactions, did not erase the original $^{187}\text{Os}/^{188}\text{Os}$
466 heterogeneity of the peridotite source (González-Jiménez *et al.* 2013a). Indeed, the
467 results of this study highlights the complexity of the mechanism of formation of the
468 chromites in the oceanic mantle, which may require the fractional extraction and/or
469 stepped pooling of melts for the preservation of the Os signatures during the mingling
470 process necessary to crystallise chromite (González-Jiménez *et al.* 2013a).

471 *A new geodynamic framework for the mafic-ultramafic rocks of the Chilean Coastal*
472 *Cordillera*

473 The structure of the present western margin of the South American continent is
474 seen as the result of the amalgamation of several tectonostratigraphic terranes to the
475 southern Andean margin during the Palaeozoic (Ramos *et al.* 1986; Bahlburgh *et al.*
476 1994; Ramos 2008, 2009; Bahlburgh *et al.* 2009). During the early to middle
477 Devonian the hypothetical exotic terrane known as Chilenia (Ramos *et al.* 1984;
478 Ramos and Basei 1997; Keppie and Ramos 1999) was separated from Laurentia and
479 later accreted to the proto-Andean margin in the south-central part of Chile (Ramos *et*
480 *al.* 1986; Davis *et al.* 2000; Ramos 2008). The continental crust of the Chilenia micro-
481 continent was later intruded by the Southern Coastal Batholith ca. 295-307 Ma ago
482 (Hervé *et al.* 1988, 2013; Lucassen *et al.* 2004; Glodny *et al.* 2008). The geochemical
483 and isotopic studies indicate that the parental melts of these intrusive rocks were
484 derived from a portion of sub-arc mantle overlying a supra-subduction zone
485 (Lucassen *et al.* 2004). These observations lead us to suggest that this section of the
486 paleo-margin of Gondwana remained as a passive margin until the early Late
487 Carboniferous when a paleo-subduction zone was initiated (Fig. 9). This
488 interpretation is consistent with previous hypotheses that the paleomargin of
489 Gondwana was a passive margin from Ordovician to Early Carboniferous time (Hervé
490 *et al.* 1987; Bahlburg and Hervé 1997; Augustsson and Balhburg 2003). The
491 formation of sedimentary rocks that now constitute the Western Series is related to the
492 erosion of amalgamated terranes, as is indicated by the U-Pb ages of detrital zircons
493 in these units (Hervé *et al.* 2013).

494 Rapalini and Vilas (1991) suggested that between the Late Carboniferous and the
495 Early Permian, the vector of subduction of the proto-Pacific changed to a northward
496 oblique direction, which resulted in the rotation of several continental blocks with
497 strike-slip displacement parallel to the western continental margin of South America.
498 This interpretation, based on paleomagnetic studies, is consistent with the fact that the
499 Lanalhue Faut zone acted, in its initial stages of development, as a ductile
500 deformation zone with divergent character (Glodny *et al.* 2008). We suggest that this
501 change of the tectonic regime, which very likely also increased the angle of the
502 subducting slab, coupled with the associated rollback of the subducting plate,
503 enhanced the break-up of a portion of Chilenia by opening of a marginal basin in the
504 fore-arc region (Fig. 9).

505 The emplacement of the La Cabaña peridotites into the continental crust is poorly
506 constrained at 282 ± 6 Ma, based on K-Ar dating of fuchsite, whereas granitoids
507 intruded the continental crust of Chilenia ca. 295-307 Ma. This suggests that this
508 marginal basin was active for a very short period (~10 Ma). Interestingly, the Os
509 isotopic values of the studied chromites are also within the range of values determined
510 for the subcontinental lithospheric mantle near the studied area, determined by the
511 analyses of mantle xenoliths located in the back-arc region of the Andes (Schilling *et*
512 *al.* 2008). This suggest that peridotites that are representative of ancient SCLM
513 beneath Chilenia could have become part of an oceanic basin being altered (i.e.,
514 oceanised), and later served as the basement for the accumulation of oceanic basalts
515 and sediments, similar to that observed in other oceanic basins (Tsuru *et al.* 2000; Shi
516 *et al.* 2007; 2013; Griffin *et al.* 2009; O'Reilly *et al.* 2009; Tang *et al.* 2013). This
517 marginal basin very likely developed in a fore-arc position and must have been
518 limited to the west by a fragment of the former Chilenia terrain (Fig. 9). Additional
519 evidence for the formation of this marginal basin is provided by the geochemistry of
520 the chromitites presented here, and the E-MORB signature of the metabasites
521 widespread through the Western Series (Díaz *et al.* 1988; Vivallo *et al.* 1988; Rabbia
522 *et al.* 1994; Hufmann and Massone 2000). This interpretation is also consistent with
523 the presence of several Besshi-type massive sulfide deposits interpreted as formed in
524 a proximal setting in a marginal basin (Alfaro and Collao 1990; Schira *et al.* 1990). In
525 this new model, the protolithic sedimentary rocks of the Western Series resulted from
526 erosion and later sedimentation within the marine basin of Carboniferous granitic
527 plutons and possibly some parts of the previously-formed Eastern Series (Fig. 9).

528 A compressive regime can be related with the San Rafael orogeny, as described by
529 Mpodozis and Kay (1990, 1992) for the northern part of Chile (28° - 31° S), in which a
530 hypothetical terrane (Terrane X) collided with the Chilean paleo-Pacific margin
531 during the Early Permian. In an analogous way, the proposed separated fragment of
532 Chilenia docked with the Gondwana margin, producing the Early Permian
533 metamorphism preserved in the rocks of both Western and Eastern Series (Höfer *et al.*
534 2001; Glodny *et al.* 2008). We currently lack evidence for this fragment of Chilenia,
535 which may have been lost by tectonic erosion associated with subduction.

536

537 **Conclusions**

- 538 (1) The geochemistry signature of the La Cabaña chromitites suggests that they
539 precipitated from arc-type melts originated within a suprasubduction zone
540 environment. This new interpretation rules out previous models that have
541 suggested that the mafic and ultramafic rocks of the Coastal Cordillera were
542 formed in an abyssal setting.
- 543 (2) The initial $^{187}\text{Os}/^{188}\text{Os}$ ratios for four chromitite samples, calculated for the
544 estimated age of emplacement, range from 0.1248 to 0.1271. These isotopic
545 compositions are within the worldwide range of reported Re-Os data for
546 chromitites from other Phanerozoic ophiolites.
- 547 (3) The formation of the chromitites was associated with the formation and
548 evolution of a marginal basin above the supra-subduction zone. However,
549 unlike most chromitites reported worldwide, this basin did not develop behind
550 an island arc but in a fore-arc setting. Available regional data suggest that they
551 originated in a pull-apart basin that separated a portion of the Chilenia micro-
552 continent. The opening of this marginal basin was associated with the change
553 in the direction of subduction in the paleo-Pacific subduction zone, and
554 involved the “oceanisation” of the old subcontinental lithospheric mantle.
555

556 **Acknowledgements**

557 The authors are grateful to the Editor, Robert J. Stern for editorial handling, and two
558 anonymous referees for their constructive criticisms, which greatly improved our
559 manuscript. We thank Prof. William L. Griffin, Macquarie University, Australia for
560 his review of an earlier version of this manuscript. This research was funded by
561 FONDECYT project #1110345 and the project CGL2010-15171 funded by the
562 Spanish Ministry of Education and Science.
563

564 **Figure captions**

565
566 **Figure 1.** Geological sketch map of the Coastal Cordillera of south-central Chile with
567 the location of the La Cabaña area (modified from SERNAGEOMIN, 2003)
568

569 **Figure 2.** Simplified geological map of the La Cabaña area (modified from Höfer *et*
570 *al.* 2001) showing the location of chromitite bodies observed *in situ* and collected
571 from the rainforest drainage network. Legend is inset in the figures.
572

573 **Figure 3.** Photographs showing morphologies and structures of the studied
574 chromitites in the La Cabaña ultramafic bodies. (a), (b) and (c) are chromitites
575 observed *in situ* at Lavanderos whereas (d) and (e) are boulders of chromitite
576 collected from the rainforest drainage network. In photographs (b) and (c) late
577 chrysotile (Ctl) veins in disrupt in the chromitite. The size of the different objects
578 shown in the figures for scale are: pen in (a) 15 cm long, coins in (b) and (c) 2 cm and
579 2.3 cm in diameter respectively, and hammer in (d) and (e) 35 cm.

580
581 **Figure 4.** Back-scattered electron (BSE) images showing textures of chromitites of
582 the La Cabaña area. (a) chromite grain completely transformed to secondary porous
583 chromite at Lavanderos, (b) partly altered chromite with porous chromite rim and
584 homogenous unaltered core at Centinela Bajo. We use the definition of porous
585 chromite and partly altered chromite micro-structures as defined [Gervilla et al.](#)
586 (2012).

587
588 **Figure 5.** Chemistry of primary chromite (black circles) of the Centinela Bajo
589 chromitite as comparison with chromian spinel of various tectonic settings in terms of
590 (a) Al-Cr-Fe³⁺ compositions, (b) TiO₂ versus Cr₂O₃. (c) Cr# [Cr/(Cr+Al)] versus Mg#
591 [Mg/(Mg+Fe)]. (d) TiO₂ versus Al₂O₃. Data sources for chromian spinel of different
592 tectonic settings taken from [Kamenetsky et al. \(2001\)](#) and [Proenza et al. \(2007\)](#).

593
594 **Figure 6.** C1-chondrite ([Naldrett and Duke 1980](#)) normalised patterns of the La
595 Cabaña chromitite and comparison with the chromitites hosted in the ophiolitic
596 mantle ([Proenza et al. 2007 and references therein](#)) and in Alaskan-type complexes
597 ([Garuti et al. 2003, 2005](#)) of the Urals and Bushveld (UG2) Layered Complex
598 ([Naldrett et al. 2011](#)). Other selected chromitites (with high-Cr and high-Al chromite)
599 of Latin America have been included for comparison: Vizcaino, Baja California Sur,
600 Mexico ([Vatin-Perigon et al. 2000](#)); Tehuitzingo, Acatlan Complex, Mexico ([Proenza](#)
601 [et al. 2004](#)); Pampean Ranges, Argentina ([Escayola et al. 2004](#)); Santa Elena, Costa
602 Rica ([Zaccarini et al. 2011](#)); Sagua de Tánamo, Mayarí-Baracoa ophiolite, Cuba
603 ([González-Jiménez et al. 2011](#)).

604
605 **Figure 7.** Initial ¹⁸⁷Os/¹⁸⁸Os versus presumed age (Ga) of ophiolite formation for the
606 La Cabaña chromitites and other chromitites hosted in the mantle section of
607 Phanerozoic SSZ ophiolites. Here the term “age of ophiolite formation” is considered
608 as either timing of the incorporation of the peridotite substrate into an “oceanic”
609 column, with an overlay of basaltic and gabbroic crust and sediments, or the time
610 when the crust-mantle sequence was emplaced onto the continental crust for
611 preservation. The gray line represents the evolution trajectory for the primitive upper
612 mantle (PUM) as reported by [Meisel et al. \(2001\)](#) whereas black one corresponds to
613 estimates for chromitites worldwide ([Walker et al. 2002b](#)). The plot (a) for whole-
614 rock and chromite separates includes data reported by [Walker et al. \(2002b\)](#) for
615 chromitites worldwide ophiolite as well as data for Albania ([Kocks et al. 2007](#));
616 Kraubath, Austria ([Melcher and Meisel 2004](#)); Shetland, Scotland ([Walker et al.](#)
617 [2002b](#); [O’Driscoll et al. 2012](#)); Mayarí-Baracoa, Cuba ([Gervilla et al. 2005](#); [Frei et al.](#)
618 [2006](#)); Mugla, Turkey ([Uysal et al. 2009](#)); and Sartohay, China ([Shi et al. 2012](#)). The
619 plot (b) includes data for *in-situ* PGM and BMS analysed in chromitites from the
620 Eastern Desert, Egypt ([Ahmed et al. 2006](#)); Dobromiritsi, Bulgaria ([González-Jiménez](#)
621 [et al. 2013b](#)); Kraubath, Austria ([Malitch 2004](#)), Loma Baya, Mexico ([González-](#)
622 [Jiménez et al. 2014a](#)); Luobusa and Donqiao, Tibet ([Shi et al. 2007](#)); Mayarí and

623 Sagua de Tánamo, Cuba (Marchesi *et al.* 2011; González-Jiménez *et al.* 2012a),
624 Oman (Ahmed *et al.* 2006); and the Ojén Lherzolite Massif, Spain (González-Jiménez
625 *et al.* 2013a). Note the smoothing effect of bulk-chromite data compared to the *in-situ*
626 analyses of individual PGM and BMS, as several generations of the latter control the
627 budget of Os-isotopes in the chromitite.

628

629

630 **Figure 8.** NiO versus Mg# in olivine relicts in dunites of Centinela Bajo; these are
631 very similar to those in ultra-depleted peridotites of the Cuban ophiolites (Proenza *et*
632 *al.* 1999).

633 **Figure 9.** Geodynamic model proposed for the evolution of the Chilean Coastal
634 Cordillera.

635

636 **Tables**

637

638 **Table 1.** Selected analyses of unaltered chromite cores of Centinela Bajo chromitites

639 **Table 2.** Platinum-group elements of chromitite samples from the La Cabaña
640 ultramafic bodies.

641 **Table 3.** Re and Os isotopes and abundances of selected chromitite samples from the
642 La Cabaña ultramafic bodies.

643

644 **References**

645

646 Aguirre, L., Hervé, F., and Godoy, E., 1972, Distribution of metamorphic facies in Chile, an
647 outline: *Kristalinikum*, v. 9, p 7–19.

648 Ahmed, A.H., and Arai, S., 2002. Unexpectedly high-PGE chromitite from the deeper mantle
649 section of the Oman ophiolite and its tectonic implications. *Contributions to Mineralogy*
650 *and Petrology*, v. 143, p. 263-278.

651 Ahmed, A.H., Hanghøj, K., Kelemen, P.B., Hart, S.R., and Arai, S., 2006, Osmium isotope
652 systematics of the Proterozoic and Phanerozoic ophiolitic chromitites: in situ ion probe
653 analysis of primary Os-rich PGM. *Earth and Planetary Science Letters*, v. 245, p. 777–791.

654 Alfaro, G., 1980, Antecedentes preliminares sobre la composición y génesis de las cromitas
655 de La Cabaña (Cautín). *Revista Geológica de Chile*, v. 11, p. 29-41.

656 Alfaro, G., and Collao, S., 1990, Massive Sulfides in the Greenstone Belt of South-Central
657 Chile – An Overview. In: FONTBOTÉ, L., AMSTUTZ, G. C., CARDOZO, M.,

- 658 CEDILLO, E. & FRUTOS, J. (eds) *Stratabound Ore Deposits in the Andes*. Springer,
659 Berlin, 199-208
- 660 Andrews, D.R.A., and Brenan, J.M., 2002, Phase-equilibrium constraints on the magmatic
661 origin of laurite and Os–Ir alloy. *Canadian Mineralogist* v. 40, p. 1705–1716.
- 662 Augé, T., 1987, Chromite deposits in the northwestern Oman ophiolite: mineralogical
663 constraints. *Mineralium Deposita*, v. 22, p. 1–10.
- 664 Augustsson, C., and Bahlburg, H., 2003, Active or passive continental margin? Geochemical
665 and Nd isotope constraints of metasediments in the backstop of a pre-Andean accretionary
666 wedge in southernmost Chile (46°30′–48°30′S). In: MCCANN, T. & SAINTOT, A. (eds)
667 *Tracing Tectonic Deformation Using the Sedimentary Record*. Geological Society,
668 London, Special Publications, v. 208, p. 253–268.
- 669 Bahlburg, H., and Hervé, F., 1997, Geodynamic evolution and tectonostratigraphic terranes of
670 northwestern Argentina and northern Chile. *GSA Bulletin*, v. 109, p. 869–884.
- 671 Bahlburg, H., Moya, C., and Zeil, W., 1994, Geodynamic evolution of the early Palaeozoic
672 continental margin of Gondwana in the Southern Central Andes of Northwestern
673 Argentina and Northern Chile. In: REUTTER, K.-J., SCHEUBER, E. & WIGGER, P.
674 (eds) *Tectonics of the Southern Central Andes*. Springer, Berlin, p. 293–302.
- 675 Bahlburg, H., Vervoort, J.D., Du frane, S.A., Bock, B., Augustsson, C., and Reimann, C.
676 2009, Timing of crust formation and recycling in accretionary orogens: Insights learned
677 from the western margin of South America. *Earth-Science Reviews*, v. 97, p. 215-241.
- 678 Barra F., Gervilla, F., Hernández, E., Reich, M. and Padrón-Navarta J. A. (in press) Alteration
679 patterns of chromian spinels from La Cabaña peridotite, south-central Chile:
680 Considerations on the formation of ferritchromite. *Mineralogy and Petrology*.
- 681 Barra, F., Rabbia, O.M., Alfaro, G., Miller, H., Hofer, C., and Kraus, S., 1998, Serpentinitas y
682 cromititas de La Cabaña, Cordillera de la Costa, Chile central. *Revista Geológica de Chile*,
683 v. 25, p. 29-44.
- 684 Birck, J.-L., Roy-Barman, M., and Capmas, F., 1997, Re–Os isotopic measurements at the
685 femtomole level in natural samples. *Geostandards Newsletter*, v. 20, p. 9–27.
- 686 Bockrath, C., Ballhaus, C., and Holzheid, A., 2004, Stabilities of laurite RuS₂ and
687 monosulphide liquid solution at magmatic temperature. *Chemical Geology*, v. 208, p.
688 265–271.
- 689 Braun, M.G., and Kelemen, P.B., 2002, Dunite distribution in the Oman Ophiolite:
690 implications for melt flux through porous dunite conduits. *Geochemistry, Geophysics*,

691 Geosystems 3 (11), 8603. <http://dx.doi.org/10.1029/2001GC000289>.

692 Brenan, J.M., and Andrews, D., 2001, High-temperature stability of Laurite and Ru–Os–Ir
693 alloy and their role in PGE fractionation in mafic magmas. *The Canadian Mineralogist*, v.
694 39, p. 341–360.

695 Büchl, A., Brüggemann, G., and Batanova, V.G., 2004. Formation of podiform chromitite
696 deposits: implications from PGE abundances and Os isotopic compositions of chromitites
697 from the Troodos complex, Cyprus. *Chemical Geology*, v. 208, p. 217-232.

698 Cohen, A. S., and Waters F. G., 1996, Separation of osmium from geological materials by
699 solvent extraction for analysis by TIMS. *Analytica Chimica Acta*, v. 332, p. 269–275.

700 Crawford, A.J., Fallon, T.J., and Green, D.H., 1989, Classification, petrogenesis and tectonic
701 setting of boninites. In: Crawford, A.J. (Ed.), *Unwin and Hyman*, London, pp. 2–44

702 Dahlquist, J.A., Rapela, C.W., Pankhurst, R.J., Fanning, C.M., Vervoort, J.D., Hart, G.,
703 Baldo, E.G., Murra, J.A., Alasino, P.H., and Colombo, F., 2012, Age and magmatic
704 evolution of the Famatinian granitic rocks of Sierra de Ancasti, Sierras Pampeanas, NW
705 Argentina. *Journal of South American Earth Sciences*, v. 34, p. 10-25.

706 Dare, S.A.S., Pearce, J.A., McDonald, I., and Styles, M.T., 2009, Tectonic discrimination of
707 peridotites using fO_2 –Cr# and Ga–Ti–Fe^{III} systematics in chrome–spinel. *Chemical*
708 *Geology*, v. 261 (3–4), p. 199-216.

709 Davis, J., Roeske, S.M., McClelland, W.C., and Kay, S.M., 2000, Mafic and ultramafic
710 crustal fragments of the southwestern Precordillera terrane and their bearing on tectonic
711 models of the early Paleozoic in western Argentina. *Geology*, v. 28, p. 171–174.

712 Díaz, L., Vivallo, W., Alfaro, G., and Cisternas M. E. 1988, Geoquímica de los esquistos
713 paleozoicos de Bahía Mansa, Osorno, Chile. In: *Congreso Geológico Chileno No. 5*,
714 *Actas*, E75-E96. Santiago, Chile.

715 Escayola, M., Proenza, J.A., Schalamuk, A., and Cábana, C., 2004. La secuencia ofiolítica de
716 la faja ultramáfica de Sierras Pampeanas de Córdoba, Argentina. In: Pereira, E.,
717 Castroviejo, R., Ortiz, F. (Eds.), *Complejos ofiolíticos en Iberoamérica*, Proyecto XIII.1—
718 *CYTED*, pp. 133–155.

719 Escayola, M., Garuti, G., Zaccarini, F., Proenza, J.A., Bédard, J.H., and Van Staal, C., 2011.
720 Chromitite and platinum-group-element mineralization at Middle Arm Brook, central
721 Advocate Ophiolite Complex, Baie Verte peninsula, Newfoundland, Canada. *The*
722 *Canadian Mineralogist*, v. 49, p. 1523-1547.

- 723 Forsythe, R., 1982, The late Paleozoic and Early Mesozoic evolution of southern South
724 America: A plate tectonic interpretation. *Journal of the Geological Society of London*, v.
725 139, p. 671–682.
- 726 Frei, R., Gervilla, F., Meibom, A., Proenza, J.A., and Garrido, C.J., 2006, Os isotope
727 heterogeneity of the upper mantle: evidence from the Mayarí–Baracoa ophiolite belt in
728 eastern Cuba. *Earth and Planetary Science Letters*, v. 241, p. 466–476.
- 729 Frutos, J., and Alfaro, G., 1987, Metallogenic and tectonic characteristics of the Paleozoic
730 ophiolitic belt of the southern Chile Coastal Cordillera. *Geologische Rundschau*, v. 76, p.
731 343-356.
- 732 Galdames, C., Rabbia, O.M., Alfaro, G., and Hernández, L., 2011, Platinum-Group Elements
733 in Ultramafic Rocks from La Cabaña Area, Coastal Cordillera of South-Central Chile. 11th
734 International Platinum Symposium. Ontario Geological Survey, Miscellaneous Release–
735 Data 269.
- 736 Garuti, G., Zaccarini, F., Moloshag, V., and Alimov, V., 1999, Platinum-group elements as
737 indicators of sulphur fugacity in ophiolitic upper mantle: an example from chromitites of
738 the Ray-Iz ultramafic complex, Polar Urals, Russia. *The Canadian Mineralogist*, v. 37, p.
739 1099–1115.
- 740 Garuti, G., Puskarev, E.V., Zaccarini, F., Cabella, R., and Anikina, E.V., 2003, Chromite
741 composition and platinum-group mineral assemblage in the Uktus Alaskan type complex
742 (central Urals, Russia). *Mineralium Deposita*, v. 38, p. 312–326.
- 743 Garuti, G., Pushkarev, E., and Zaccarini, F., 2005, Diversity of chromite-PGE mineralization
744 in ultramafic complexes of the Urals. In: Törmänen, T.O., Alapieti, T.T. (Eds.), *Platinum-*
745 *group elements—from genesis to beneficiation and environmental impact*. Tenth Int.
746 *Platinum Symposium (Oulu)*, pp. 341–344.
- 747 Gervilla, F., Proenza, J.A., Frei, R., González-Jiménez, J.M., Garrido, C.J., Melgarejo, J.C.,
748 Meibom, A., Díaz-Martínez, R., and Lavaut, W., 2005, Distribution of platinum-group
749 elements and Os isotopes in chromite ores from Mayarí–Baracoa Ophiolite Belt (eastern
750 Cuba). *Contributions to Mineralogy and Petrology*, v. 150, p. 589–607.
- 751 Gervilla, F., Padrón-Navarta, J.A., Kerestedjian, T., Sergeeva, I., González-Jiménez, J.M.,
752 and Fanlo, I., 2012, Formation of ferrian chromite in podiform chromitites from the
753 Golyamo Kamenyane serpentinite, Eastern Rhodopes, SE Bulgaria: a two-stage process.
754 *Contributions to Mineralogy and Petrology*. <http://dx.doi.org/10.1007/s00410-012-0763-3>.
- 755 Ghosh, B., Pal, T., Bhattacharya, A., and Das, D., 2009, Petrogenetic implications of
756 ophiolitic chromite from Rutland Island, Andaman—a boninitic parentage in supra-

757 subduction setting. *Mineralogy and Petrology*, v. 96, p. 59-70. DOI: DOI 10.1007/s00710-
758 008-0039-9.

759 Glodny, J., Lohrmann, J., Echtler, H., Gräfe, K., Seifert, W., Collao, S., and Figueroa, O.,
760 2005, Internal dynamics of a paleoaccretionary wedge: insights from combined isotope
761 tectonochronology and sandbox modelling of the south-central Chilean forearc. *Earth and*
762 *Planetary Science Letters*, v. 231, p. 23–39.

763 Glodny, J., Echtler, H., Collao, S., Ardiles, M., Burón, P., and Figueroa, O., 2008,
764 Differential Late Paleozoic active margin evolution in South-Central Chile (37°S–40°S) –
765 the Lanalhue Fault Zone. *Journal of South American Earth Sciences*, v. 26, p. 397-411

766 Godoy, E., and Kato, T., 1990, Late Palaeozoic serpentinites and mafic schists from the Coast
767 Range accretionary complex, central Chile: their relation to aeromagnetic anomalies.
768 *Geologische Rundschau*, v. 79, p. 121–130.

769 González-Jiménez, J.M., Proenza, J.A., Gervilla, F., Melgarejo, J.C., Blanco-Moreno, J.A.,
770 Ruiz- Sánchez, R., and Griffin, W.L., 2011, High-Cr and high-Al chromitites from the
771 Sagua de Tánamo district, Mayarí-Cristal Ophiolitic Massif (eastern Cuba): constraints on
772 their origin from mineralogy and geochemistry of chromian spinel and platinum-group
773 elements. *Lithos*, v. 125, p. 101–121.

774 González-Jiménez, J.M., Gervilla, F., Griffin, W.L., Proenza, J.A., Augé, T., O'Reilly, S.Y.,
775 and Pearson, N.J., 2012a, Os-isotope variability within sulfides from podiform
776 chromitites. *Chemical Geology*, v. 291, p. 224–235.

777 González-Jiménez, J.M., Griffin, W.L., Gervilla, F., Kerestedjian, T.N., O'Reilly, S.Y., and
778 Proenza, J.A., Pearson, N.J., Sergeeva, I., 2012b, Metamorphism disturbs the Re–Os
779 signatures of platinum-group minerals in ophiolite chromitites. *Geology*.
780 <http://dx.doi.org/10.1130/G33064.1>.

781 González-Jiménez, J.M., Marchesi, C., Griffin, W.L., Gutiérrez-Narbona, R., Lorand, Jean.-P.,
782 O'Reilly, S.Y., Garrido, C.J., Gervilla, F., Pearson, N.J., and Hidas, K., 2013a, Transfer of
783 Os isotopic signatures from peridotite to chromitite in the subcontinental mantle: insights
784 from in situ analysis of platinum-group and base-metal minerals (Ojén peridotite massif,
785 southern Spain). *Lithos*, v. 164-167, p. 74-85.

786 González-Jiménez, J.M., Locmelis, M., Belousova, E., Griffin, W.L., Gervilla, F.,
787 Kerestedjian, T.N., Pearson, N.J., and Sergeeva, I., 2013b, Genesis and tectonic
788 implications of podiform chromitites in the metamorphosed Ultramafic Massif of
789 Dobromirski (Bulgaria). *Gondwana Research*, DOI:
790 <http://dx.doi.org/10.1016/j.gr.2013.09.020>

791 González-Jiménez, J.M., Griffin, W.L., Gervilla, F., Proenza, J.A., O'Reilly, S.Y., and
792 Pearson, N.J., 2014a, Chromitites in ophiolites: How, where, when, why? Part I. A review
793 and new ideas on the origin and significance of platinum-group minerals. *Lithos*, v. 189, p.
794 127-139.

795 González-Jiménez, J.M., Griffin, W.L., Proenza, J.A., Gervilla, F., O'Reilly, S.Y., Akbulut,
796 M., Pearson, N.J., and Arai, S., 2014b, Chromitites in ophiolites: How, where, when, why?
797 Part II. The crystallization of chromitites. *Lithos*, v. 189, 140-158.

798 Graham, I.T., Franklin, B.J., and Marshall, B., 1996, Chemistry and mineralogy of podiform
799 chromitite deposits, southern NSW, Australia: a guide to their origin and evolution.
800 *Mineralogy and Petrology*, v. 37, p. 129–150.

801 Griffin, W.L., O'Reilly, S.Y., Afonso, J.C., and Begg, G.C., 2009, The composition and
802 evolution of Lithospheric mantle: a re-evaluation and its tectonic implications. *Journal of*
803 *Petrology*, v. 50 (7), p. 1185–1204. <http://dx.doi.org/10.1093/petrology/egn033>.

804 Hervé, F., 1974. Petrology of the crystalline basement Nahuelbuta Mountains, South-Central
805 Chile. PhD thesis, Hokkaido University.

806 Hervé, F., 1977, Petrology of the Crystalline Basement of the Nahuelbuta Mountains,
807 Southcentral Chile. In: ISHIKAWA, T. & AGUIRRE, L. (eds) *Comparative Studies on the*
808 *Geology of the Circum Pacific Orogenic Belt in Japan and Chile*. Japan Society for the
809 Promotion of Science, Tokyo, p.1–51.

810 Hervé, F., Davidson, J., Godoy, E., Mpodozis, C., and Covacevich, V., 1981, The Late
811 Paleozoic in Chile: stratigraphy, structure and possible tectonic framework. *Revista da*
812 *Academia do Ciencias Brasil*, v. 53, p. 361–373.

813 Hervé, F., Godoy, E., Parada, M. A., Ramos, V., Rapela, C., Mpodozis, C., and Davidson, J.
814 A., 1987, A general view of the Chilean-Argentine Andes, with emphasis on their early
815 history. In: MONGER, J. W. H. & FRANCHETEAU, J. (eds.) *Circum-Pacific Orogenic*
816 *Belts and the Evolution of the Pacific Ocean Basin*. *Geodynamics Series*, v. 18, p. 97–113.

817 Hervé, F., Munizaga, F., Parada, M. A., Brook, M., Pankhurst, R., Snelling, N., and Drake,
818 R., 1988, Granitoids of the Coast Range of central Chile: Geochronology and geological
819 setting. *Journal of South American Earth Sciences*, v. 1, p. 185–195.

820 Hervé, F., Calderón, M., Fanning, C. M., Pankhurst, R. J., and Godoy, E., 2013, Provenance
821 variations in the Late Paleozoic accretionary complex of central Chile as indicated by
822 detrital zircons. *Gondwana Research*, v. 23, p. 1122-1135

- 823 Hicky, R.L., and Frey, F.A., 1982, Geochemical characteristics of boninite series volcanic:
824 implication for their source. *Geochimica et Cosmochimica Acta*, v. 46, p. 2099-2115.
- 825 Höfer, C., Kraus, S., Miller, H., Alfaro, G., and Barra, F., 2001, Chromite-bearing
826 serpentinite bodies within an arc-backarc metamorphic complex near La Cabana, south
827 Chilean Coastal Cordillera. *Journal of South American Earth Sciences*, v. 14, p. 113–126.
- 828 Hufmann, L., and Massonne, H. 2000, Ancient arc/back-arc and N-MORB volcanics
829 incorporated in the Late Palaeozoic/Early Mesozoic metamorphic complex of the Coastal
830 Cordillera of Chiloé, Southern Central Chile. In *Congreso Geológico Chileno*, No. 9,
831 *Actas*, v. 2, p. 738-741. Puerto Varas, Chile.
- 832 Ishimaru, S., Arai, S., Ishida, Y., Shirasaka, M., and Okrugin, V.M., 2007. Melting
833 and multi-stage metasomatism in the mantle wedge beneath a frontal arc inferred
834 from highly depleted peridotite xenoliths from the Avacha Volcano, southern
835 Kamchatka. *Journal of Petrology*, v. 48, p. 395-433.
- 836 Jugo, P., 2009, Sulfur content at sulfide saturation in oxidized magmas. *Geology*, v. 37, p.
837 415-418.
- 838 Kamenetsky, V.S., Crawford, A.J., and Meffre, S., 2001, Factors controlling chemistry of
839 magmatic spinel: an empirical study of associated olivine, Cr-spinel and melt inclusions
840 from primitive rocks. *Journal of Petrology*, v. 42, p. 655–671.
- 841 Keppie, J.D., and Ramos, V.A., 1999, Odyssey of terranes in the Iapetus and Rheic oceans
842 during the Paleozoic. In: Ramos, V.A., Keppie, J.D. (eds.), *Laurentia–Gondwana*
843 *connections before Pangea: Geological Society of America Special Paper*, v. 336, p. 267–
844 276.
- 845 Kocks, H., Melcher, F., Meisel, T., and Burgath, K.P., 2007, Diverse contributing sources to
846 chromitite petrogenesis in the Shebenik Ophiolitic Complex, Albania: evidence from new
847 PGE and Os-isotope data. *Mineralogy and Petrology*, v. 91, p. 139–170.
- 848 Leblanc, M., and Nicolas, A., 1992, Les chromitites ophiolitiques: *Chronique de la Recherche*
849 *Minière*, v. 507, p. 3–25.
- 850 Leblanc, M., 1986, Chromite in ocean arc environments: New Caledonia. In: Stowe CW (ed)
851 *Evolution of chromium ore fields*. Van Nostrand Reinhold, New York, pp 265-296.
- 852 Liu, C.Z., Snow, J.E., Brüggmann, G., Hellebrand, E., and Hofmann, A.W., 2009, Non-
853 chondritic HSE budget on Earth's upper mantle evidenced by abyssal peridotites from
854 Gakkel ridge (Arctic Ocean). *Earth and Planetary Science Letters*, v. 283, p. 122-132.

- 855 Lucassen, F., Trumbull, R., Franz, G., Creixell, C., Vásquez, P., Romer, R. L., and Figueroa,
856 O., 2004, Distinguishing crustal recycling and juvenile additions at active continental
857 margins: the Paleozoic to recent compositional evolution of the Chilean Pacific margin
858 (36–41°S). *Journal of South American Earth Sciences*, v. 17, p. 103–119.
- 859 Malitch, K.N., 2004, Osmium isotope constraints on contrasting sources and prolonged
860 melting in the Proterozoic upper mantle: evidence from ophiolitic Ru–Os sulfides and Ru–
861 Os–Ir alloys. *Chemical Geology*, v. 208, p. 157–173.
- 862 Malitch, K.N., Junk, S.A., Thalhammer, O.A.R., Melcher, F., Knauf, V.V., Pernicka, E., and
863 Stumpfl, E.F., 2003, Laurite and ruarsite from podiform chromitites at Kraubath and
864 Hochgrössen, Austria: new insights from osmium isotopes. *The Canadian Mineralogist*, v.
865 41, p. 331–352.
- 866 Malpas, J., Robinson, P.T., and Zhou, M.-F., 1997, Chromite and ultramafic rock
867 compositional zoning through a paleotransform fault, Poum, New Caledonia: discussion.
868 *Economic Geology*, v. 92, p. 502–503.
- 869 Marchesi, C., Garrido, C.J., Godard, M., Proenza, J.A., Gervilla, F., and Blanco-
870 Moreno, J., 2006, Petrogenesis of highly depleted peridotites and gabbroic rocks
871 from the Mayarí-Baracoa Ophiolitic Belt (eastern Cuba). *Contributions to*
872 *Mineralogy and Petrology*, v. 151, p. 717–736.
- 873 Marchesi, C., González-Jiménez, J.M., Gervilla, F., Garrido, C.J., Griffin, W.L., O'Reilly,
874 S.Y., Proenza, J.A., and Pearson, N.J., 2011, In situ Re–Os isotopic analysis of platinum-
875 group minerals from the Mayarí–Cristal ophiolitic massif (Mayarí–Baracoa Ophiolitic
876 Belt, eastern Cuba): implications for the origin of Os-isotope heterogeneities in podiform
877 chromitites. *Contributions to Mineralogy and Petrology*, v. 161, p. 977–990.
- 878 Maurel, C., and Maurel, P., 1982, Étude expérimentale de la distribution de l'aluminium entre
879 bain silicaté basique et spinelle chromifère. Implications pétrogénétiques : teneur en
880 chrome des spinelles. *Bulletin de Minéralogie*, v. 105, p. 197–202.
- 881 Melcher, F., Grum, W., Simon, G., Thalhammer, T.V., and Stumpfl, E.F., 1997, Petrogenesis
882 of the ophiolitic giant chromite deposits of Kempirsai, Kazakhstan: a study of solid and
883 fluid inclusions in chromite. *Journal of Petrology*, v. 38, p. 1419–1458.
- 884 Meisel, T., Walker, R.J., and Morgan, 1996, The osmium isotopic composition of the Earth's
885 primitive upper mantle. *Nature*, v. 383, p. 517–520.
- 886 Meisel, T., and Melcher, F., 2004, A metamorphosed Early Cambrian Crust-Mantle
887 Transition in the Eastern Alps-Austria. *Journal of Petrology*, v. 45, p. 1689–1723.

- 888 Mpodozis, C., and Kay, S. M., 1990, Provincias magmáticas ácidas y evolución tectónica de
889 Gondwana: Andes chilenos (28–31°S). *Revista Geológica de Chile*, v. 17, p. 153–180.
- 890 Mpodozis, C., and Kay, S. M., 1992, Late Paleozoic to Triassic evolution of the Gondwana
891 margin: evidence from Chilean Frontal Cordilleran batholiths (28°S to 31°S). *Geological*
892 *Society of America Bulletin*, v. 104, p. 999–1014.
- 893 Naldrett, A., and Duke, J.M., 1980. Pt metals in magmatic sulfide ores. *Science* 208, 1417–
894 1424.
- 895 Naldrett, A.J., Wilson, A., Kinnaird, J., Yudovskaya, M., and Chunnett, G., 2011, The origin
896 of chromitites and related PGE mineralization in the Bushveld Complex: new
897 mineralogical and petrological constraints. *Mineralium Deposita*, v. 47 (3), p. 209–232.
- 898 Ohara, Y., Stern, R.J., Ishii, T., Yurimoto, H., and Yamazaki, T., 2002, Peridotites
899 from the Mariana Through: first look at the mantle beneath and active back-arc
900 basin. *Contributions to Mineralogy and Petrology*, v. 143, p. 1-18.
- 901 O’Driscoll, B., Day, J.M.D., Walker, R.J., and Daly, J.S., McDonough, W. F., Piccoli, P.M.,
902 2012, Chemical heterogeneity in the upper mantle recorded by peridotites and chromitites
903 from the Shetland Ophiolite Complex, Scotland. *Earth and Planetary Science Letters*, v.
904 333-334, p. 226-237.
- 905 O’Reilly, S.Y., Zhang, M., Griffin, W.L., Begg, G., and Hronsky, J., 2009, Ultra deep
906 continental roots and their oceanic remnants: a solution to the geochemical “mantle
907 reservoir” problem? *Lithos*, v. 112 (2), p. 1043–1054.
- 908 Pagé, P., and Barnes, S.-J., 2009, Using trace elements in chromites to constrain the origin of
909 podiform chromitites in the Thetford Mines ophiolite, Québec, Canada. *Economic*
910 *Geology*, v. 104, p. 997–1018.
- 911 Prichard, H.M., Neary, C.R., Fisher, F.C., and O’Hara, M.J., 2008, PGE-rich Podiform
912 chromitites in the Al’Ays ophiolite complex, Saudi Arabia: an example of critical mantle
913 melting to extract and concentrate PGE. *Economic Geology*, v. 103, p. 1507–1529.
- 914 Proenza, J.A., Gervilla, F., Melgarejo, J.C., and Bodinier, J.L., 1999, Al- and Cr-rich
915 chromitites from the Mayarí–Baracoa Ophiolitic Belt (Eastern Cuba): consequence of
916 interaction between volatile-rich melts and peridotites in suprasubduction mantle.
917 *Economic Geology*, v. 94, p. 547–566.
- 918 Proenza JA, Ortega-Gutiérrez, F., Camprubí, A., Tritlla, J., Elías-Herrera, M., and Reyes-
919 Salas, M., 2004, Paleozoic serpentinite-enclosed chromitites from Tehuitzingo (Acatlan

- 920 complex, southern Mexico): a petrological and mineralogical study. *Journal of South*
921 *American Earth Sciences*, v. 16, p. 649–666.
- 922 Proenza, J.A., Zaccarini, F., Lewis, J.F., Longo, F., and Garuti, G., 2007, Chromian spinel
923 composition and the platinum-group minerals of the PGE-rich Loma Peguera chromitites,
924 Loma Caribe peridotite, Dominican Republic. *The Canadian Mineralogist*, v. 45, p. 631–
925 648.
- 926 Proenza, J.A., Zaccarini, F., Escayola, M., Cábana, C., Shalamuk, A., and Garuti, G., 2008,
927 Composition and textures of chromite and platinum-group minerals in chromitites of the
928 western ophiolitic belt from Córdoba Pampeans Ranges, Argentine. *Ore Geology*
929 *Reviews*, v. 33, p. 32–48.
- 930 Rabbia, O.M., Alfaro, G., and Barra, F., 1994, Presencia de espilitas metasomatizadas en el
931 cinturón serpentinitico de la Cordillera de la Costa del sur de Chile. II Jornadas de
932 Mineralogía, Petrografía y Metalogénesis de Rocas Ultrabásicas. Universidad Nacional de
933 La Plata, Argentina, v. 3, p. 607-615.
- 934 Ramos, V. A., 2008, The Basement of the Central Andes: The Arequipa and Related
935 Terranes. *Annual Review of Earth and Planetary Sciences*, v. 36, p. 289-324
- 936 Ramos, V.A., 2009, Anatomy and global context of the Andes: Main geologic features and
937 the Andean orogenic cycle. *The Geological society of America Memoir*, v. 204, p. 31-65.
- 938 Ramos, V.A., and Basei, M., 1997, The basement of Chilenia: an exotic continental terrane to
939 Gondwana during the Early Paleozoic. *Terrane Dynamics 97*, International Conference on
940 Terrane Geology, Christchurch, New Zealand, conference abstracts, p.140–143
- 941 Ramos V.A., Jordan T., Allmendinger R.W., Kay S.M., Cortes J.M., and Palma M.A. 1984,
942 Chilenia un terreno alóctono en la evolución paleozoica de los Andes Centrales.
943 In: Congreso Geológico Argentino No 9, Actas, v. 2, p. 84–106.
- 944 Ramos, V. A., Jordan, T. E., Allmendinger, R. W., Mpodozis, C., Kay, S. M., Cortés, J. M.,
945 and Palma, 1986, Paleozoic terranes of the Central Argentine – Chilean Andes. *Tectonics*,
946 v. 5, p. 855–880.
- 947 Ramos, V., Vujovich, G., Martino, and R., Otamendi, J., 2010, Pampia: A large cratonic
948 block missing in the Rodinia supercontinent. *Journal of Geodynamics* , v. 50, p. 243–255.
- 949 Rapalini, A. E., and Vilas, J. F. 1991, Tectonic rotations in the Late Palaeozoic continental
950 margin of southern South America determined and dated by paleomagnetism. *Geophysical*
951 *Journal International*, v. 107, p. 333-351

- 952 Roberts, S., 1988, Ophiolitic chromitite formation: A marginal basin phenomenon? *Economic*
953 *Geology*, v. 83, p. 1034–1036.
- 954 Robinson, P., and Adetunji, J., 2013, The geochemistry and oxidation state of podiform
955 chromitites from the mantle section of the Oman ophiolite: a review. *Gondwana Research*.
956 DOI: <http://dx.doi.org/10.1016/j.gr.2013.07.013>
- 957 Rollinson, H.R., 2005, Chromite in the mantle section of the Oman ophiolite: a new genetic
958 model. *Island Arc*, v. 14, p. 542–550
- 959 Rollinson, H., 2008, The geochemistry of mantle chromitite from the northern part of the
960 Oman ophiolite: inferred parental melt compositions. *Contributions to Mineralogy and*
961 *Petrology*, v. 156, p. 273–288.
- 962 Schilling M., Carlson R.W., Conceicao R.V., Dantas C., Bertotto G.W., and Koester E.,
963 2008, Re-Os isotope constraints on subcontinental lithospheric mantle evolution of
964 southern South America. *Earth and Planetary Science Letters*, v. 268, p. 89-101.
- 965 Schira, W., Amstutz, G.G.C., and Fontboté, L., 1990, The Pirpen Alto Cu-(Zn) Massive
966 Sulfide Occurrence in South-Central Chile – A Kieslager-Type Mineralization in a
967 Paleozoic Ensialic Mature Marginal Basin Setting. In: FONTBOTÉ, L., AMSTUTZ, G.
968 C., CARDOZO, M., CEDILLO, E. & FRUTOS, J. (eds) *Stratabound Ore Deposits in the*
969 *Andes*. Springer, Berlin, p. 229-251.
- 970 Shi, R., Alard, O., Zhi, X., O'Reilly, S.Y., Pearson, N.J., Griffin, W.L., Zhang, M., and Chen,
971 X., 2007, Multiple events in the Neo-Tethyan oceanic upper mantle: evidence from Ru–
972 Os–Ir alloys in the Luobusa and Dongqiao ophiolitic podiform chromitites, Tibet. *Earth*
973 *and Planetary Science Letters*, v. 261, p. 33–48.
- 974 Shi, R., Griffin, W.L., O'Reilly, S.Y., Zhou, M.F., Zhao, G., Huang, Q., Zhang, X., and Ding,
975 D.L., 2012, Archean Mantle contributes to the genesis of chromitites in the Paleozoic
976 Sartohay ophiolite, Asiatic Orogenic Belt, northwestern China. *Precambrian Research*, v.
977 216-219, p. 87-94.
- 978 Shirey, S.B., and Walker, R.J., 1995, Re-Os isotopes in cosmochemistry and high-
979 temperature geochemistry. *Annual Review of Earth and Planetary Science*, v. 26, p. 423-
980 500.
- 981 Snow, J., and Reisberg, L., 1995, Os isotopic systematics of the MORB mantle: results from
982 altered abyssal peridotites. *Earth and Planetary Science Letters*, v. 133, p. 411-421.

- 983 Tang, Y.-J., Zhang, H.-F., Ying, J.-F., and Su, B.-X., 2013, Widespread refertilization of
984 cratonic and circum-cratonic lithospheric mantle. *Earth Science Reviews*, v. 118, p. 45–
985 68.
- 986 Tsuru, A., Walker, R.J., Kontinen, A., and Peltonen, P., 2000, Re–Os isotopic systematics of
987 the 1.95 Ga Jormua Ophiolite Complex, northeastern Finland. *Chemical Geology*, v.164,
988 p. 123–141.
- 989 Uysal, I., Tarkian, M., Sadiklar, M.B., Zaccarini, F., Meisel, T., Garuti, G., and Heidrich, S.,
990 2009, Petrology of Al- and Cr-rich ophiolitic chromitites from the Muğla, SW Turkey:
991 implications from composition of chromite, solid inclusions of platinum-group mineral,
992 silicate, and base-metal mineral, and Os-isotope geochemistry. *Contributions to*
993 *Mineralogy and Petrology*, v. 158, p. 659–674.
- 994 Vatin-Perignon, N., Amossé, J., Radelli, L., Keller, F., and Castro-Leyva, T., 2000, Platinum
995 group element behaviour and thermochemical constraints in the ultrabasic–basic complex
996 of the Vizcaino Peninsula, Baja California Sur, Mexico. *Lithos*, v. 53, p. 59-80.
- 997 Vergara, L. 1970. Prospección de yacimientos de cromo y hierro en La Cabaña, Cautín.
998 Bachelor's thesis. Universidad de Chile. 96 pp.
- 999 Vivallo, W., Alfaro, G., and Diaz, L. 1988, Las metabasaltos de la Serie Occidental de la
1000 Cordillera de la Costa entre los 38°-41°S latitud Sur, Chile: evidencias geoquímicas de
1001 cuenca marginal durante el Paleozoico. VII Congreso Latinoamericano de Geología
1002 (Belém), Actas, v. 1, p. 260-273.
- 1003 Walker, R.J., Horan, M.F., Morgan, J.W., Becker, H., Grossman, J.N., and Rubin, A.E.,
1004 2002a, Comparative ^{187}Re – ^{187}Os systematics of chondrites: implications regarding early
1005 solar system processes. *Geochimica et Cosmochimica Acta*, v. 66, p. 4187–4201.
- 1006 Walker, R.J., Prichard, H.M., Ishiwatari, A., and Pimentel, M., 2002b, The osmium isotopic
1007 composition of convecting upper mantle deduced from ophiolite chromites. *Geochimica et*
1008 *Cosmochimica Acta* v. 66, p. 329–345.
- 1009 Wasylenki, L.E., Baker, M.B., Kent, A.J.R., and Stolper, E.M., 2003, Near solidus melting of
1010 the shallow upper mantle: partial melting experiments on depleted peridotite. *Journal of*
1011 *Petrology*, v. 44, p. 1163–1191
- 1012 Willner, A. P., Hervé, F., and Massonne, H.-J., 2000, Mineral chemistry and pressure–
1013 temperature evolution of two contrasting highpressure–low-temperature belts in the
1014 Chonos Archipelago, Southern Chile. *Journal of Petrology*, v. 41, p. 309–330.

- 1015 Willner, A. P. 2005, Pressure-temperature evolution of an Upper Paleozoic paired
1016 metamorphic belt in Central Chile (34°–35°30'S). *Journal of Petrology*, v. 46, p. 1805–
1017 1833.
- 1018 Willner, A. P., Thomson, S. N., Kröner, A., Wartho, J., Wijbrans, J. R., and Hervé, F. 2005,
1019 Time markers for the evolution and exhumation history of a Late Paleozoic paired
1020 metamorphic belt in north-central Chile (34°–35°30pS). *Journal of Petrology*, v. 46, p.
1021 1835–1858.
- 1022 Zaccarini, F., Garuti, G., Proenza, J.A., Campos, L., Thalhammer, O.A.R., Aiglsperger, T.,
1023 and Lewis, J., 2011, Chromite and platinum-group-elements mineralization in the Santa
1024 Elena ophiolitic ultramafic nappe (Costa Rica): geodynamic implications. *Geologica Acta*,
1025 v. 9 (3–4), p. 407–423.
- 1026 Zhou, M.F., Robinson, P.T., Malpas, J., and Zijin, L., 1996, Podiform chromites in the
1027 Luobusa Ophiolite (Southern Tibet): implications for melt–rock interaction and chromite
1028 segregation in the upper mantle. *Journal of Petrology*, v. 37, p. 3–21.
- 1029 Zhou, M.F., Sun, M., Keays, R.R., and Kerrich, R.W., 1998, Controls on platinum-group
1030 elemental distributions of podiform chromitites of high-Cr and high-Al chromitites from
1031 Chinese orogenic belt. *Geochimica et Cosmochimica Acta*, p. 677-688.
- 1032

FIGURE 1.

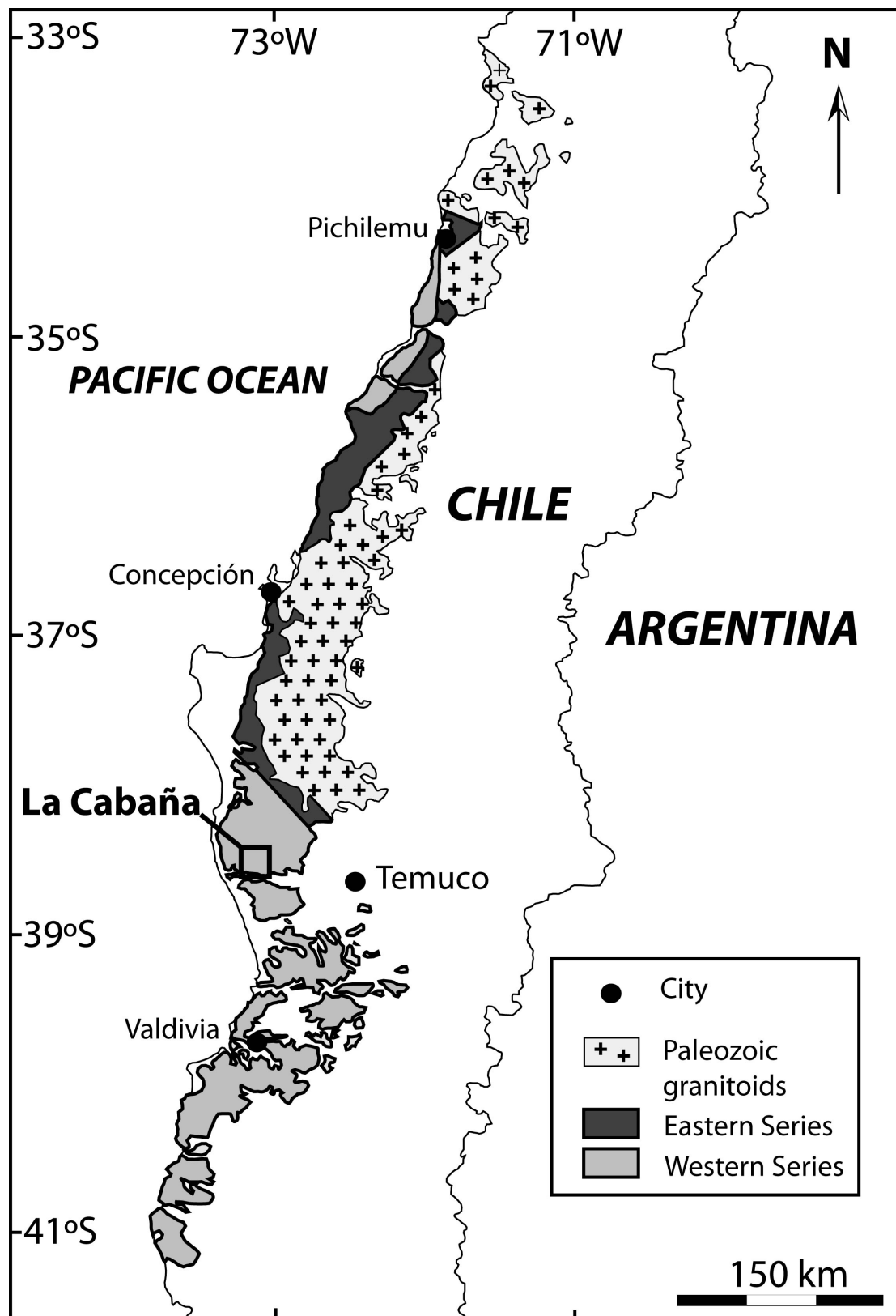


FIGURE 2.

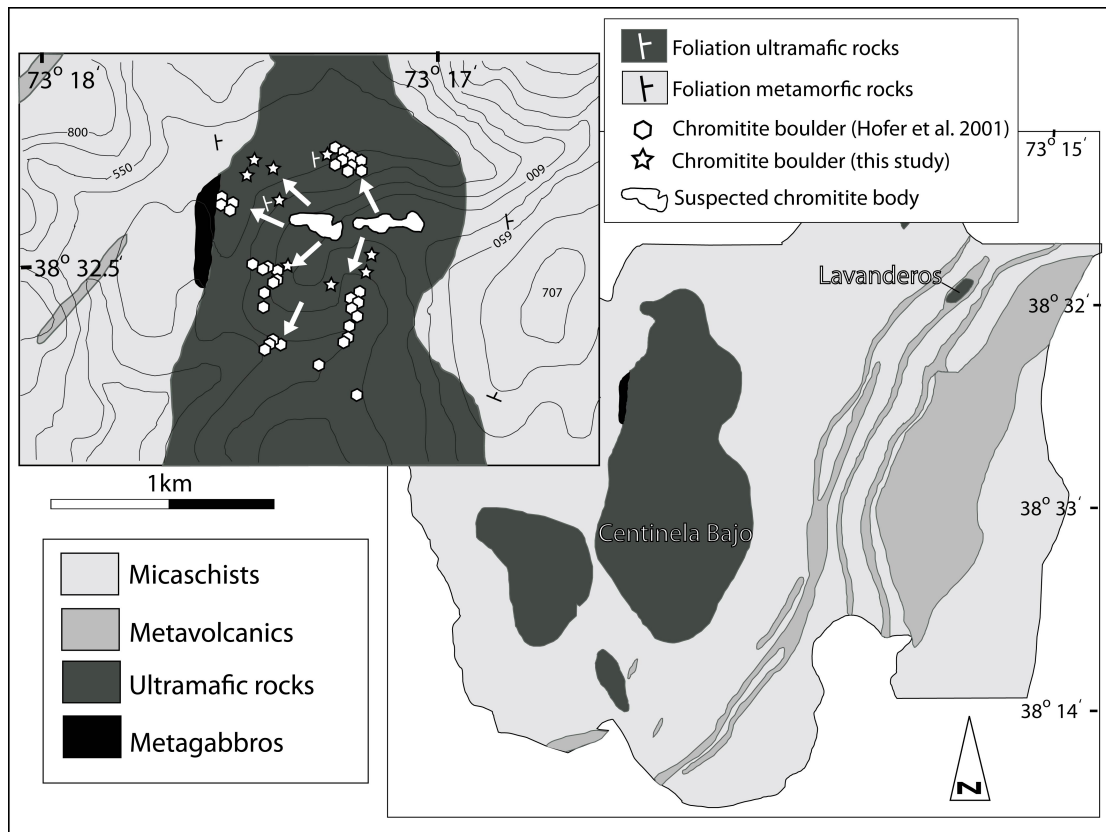


FIGURE 3.

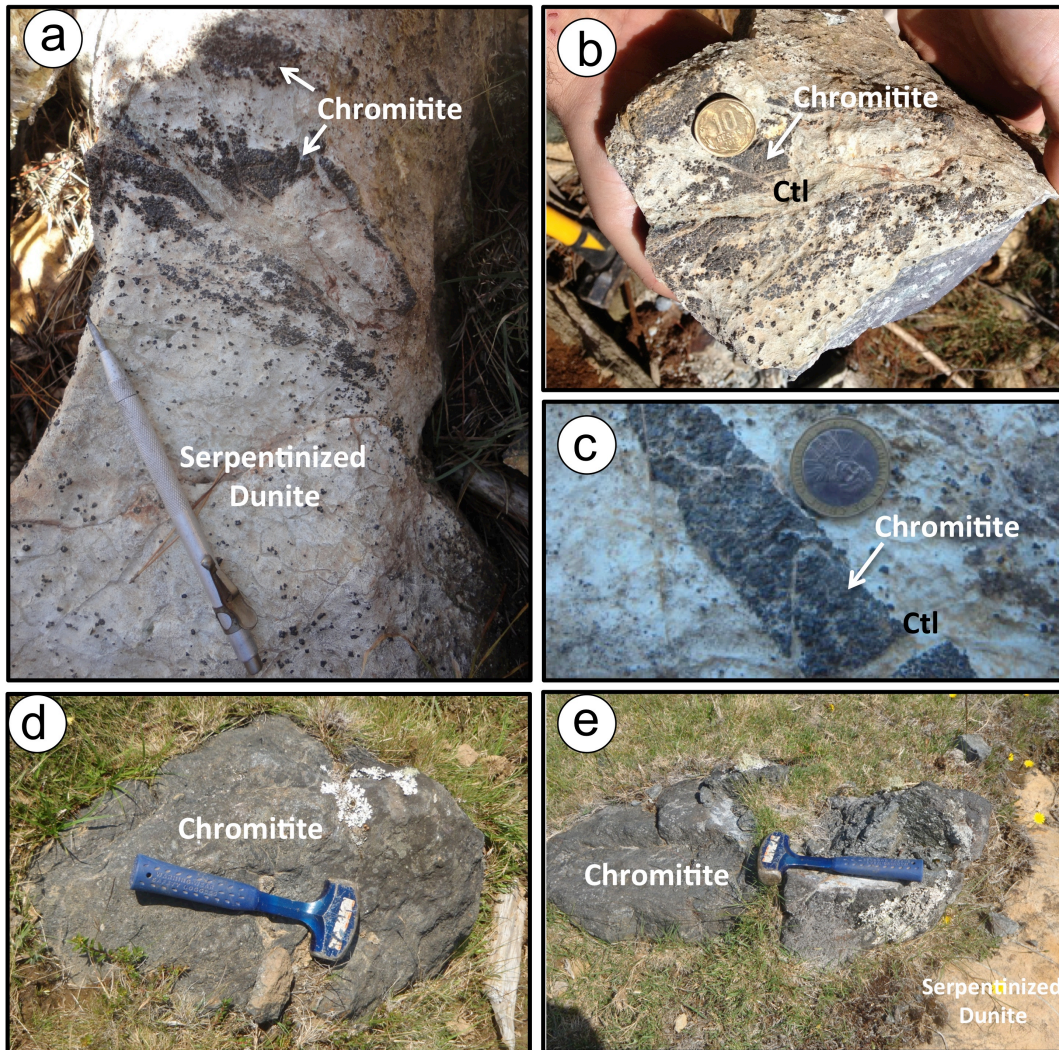


FIGURE 4.

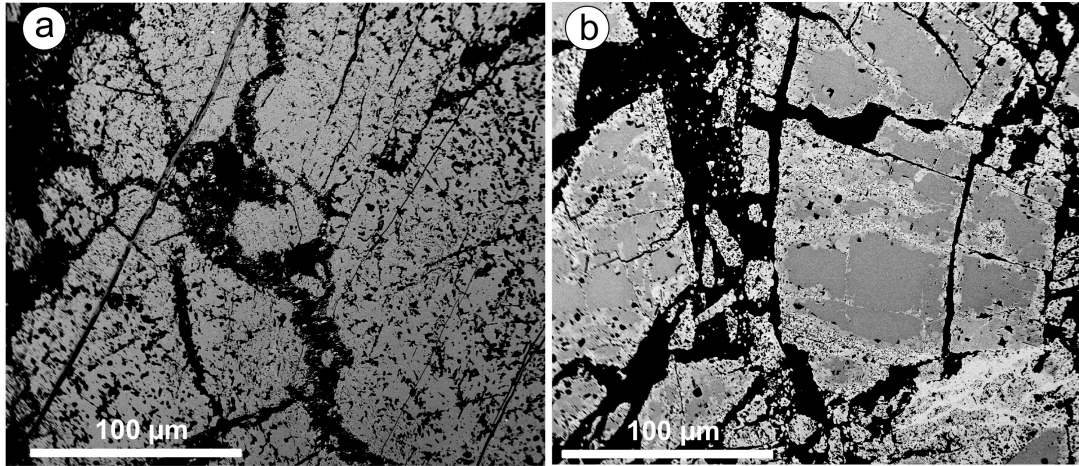


FIGURE 5.

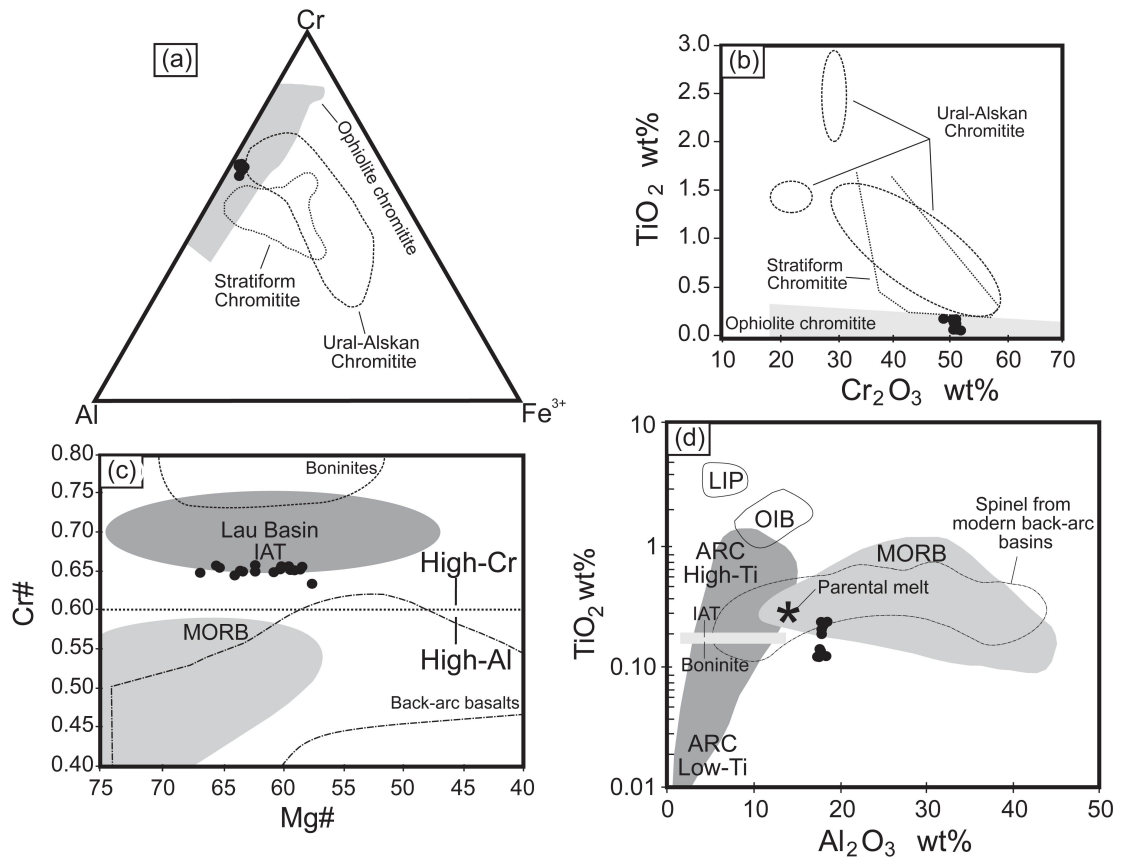


FIGURE 6

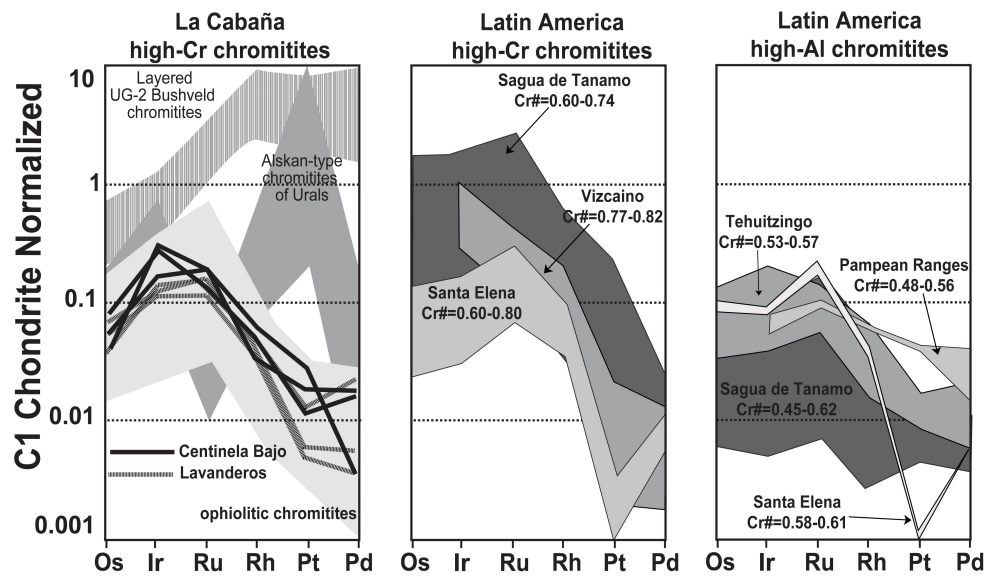
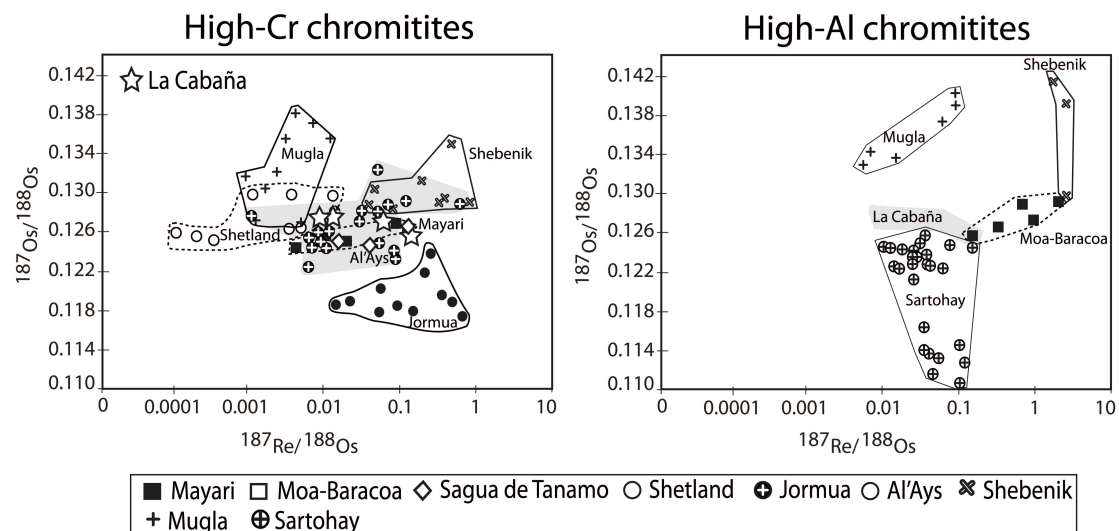


FIGURE 7.

Whole-rock chromitites



In situ PGM and BMS

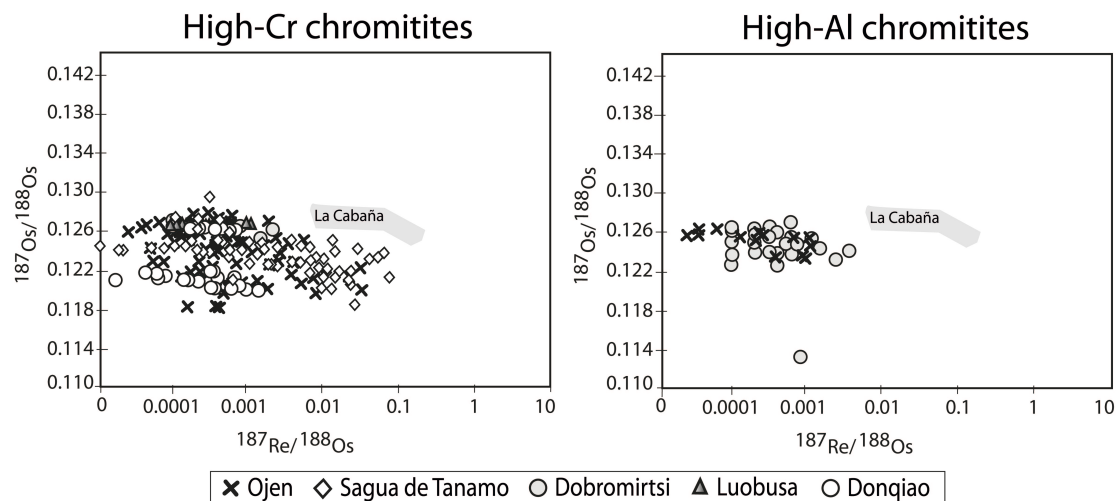


FIGURE 8.

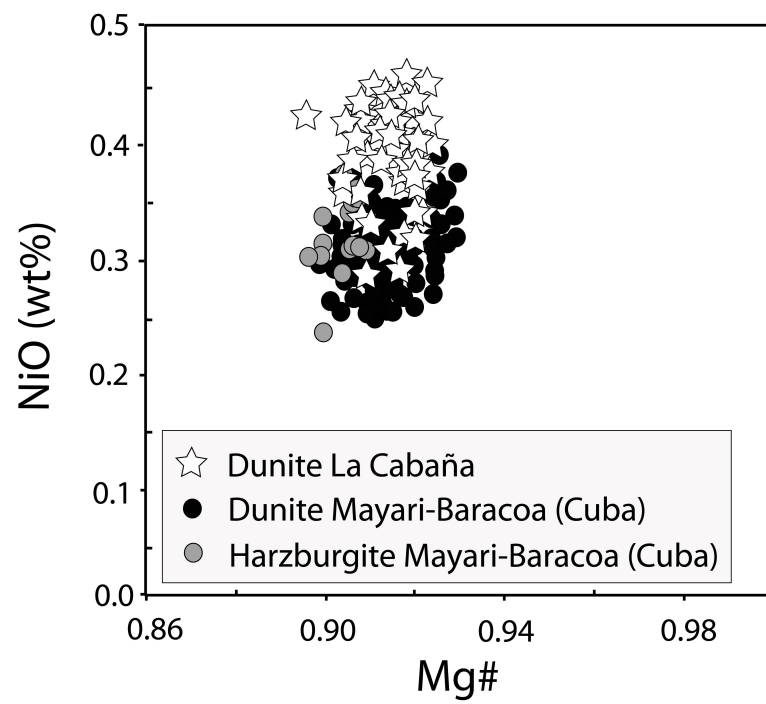
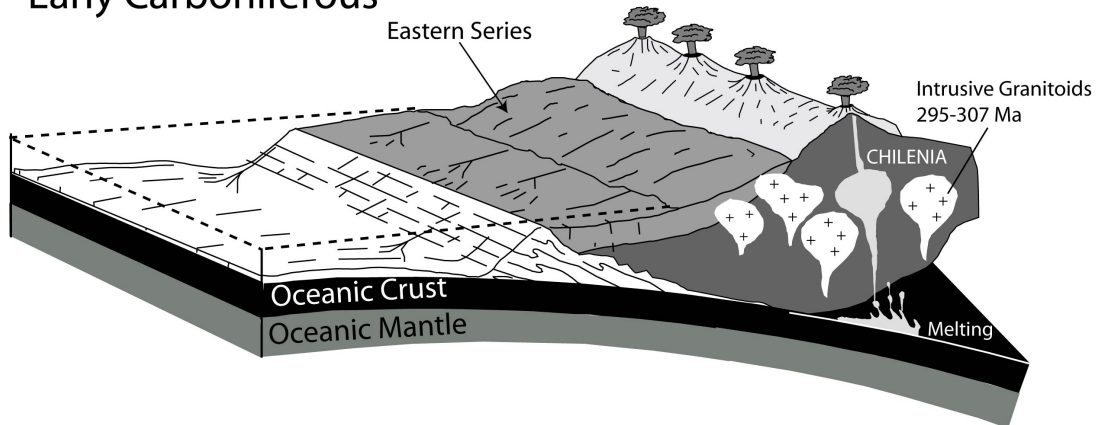
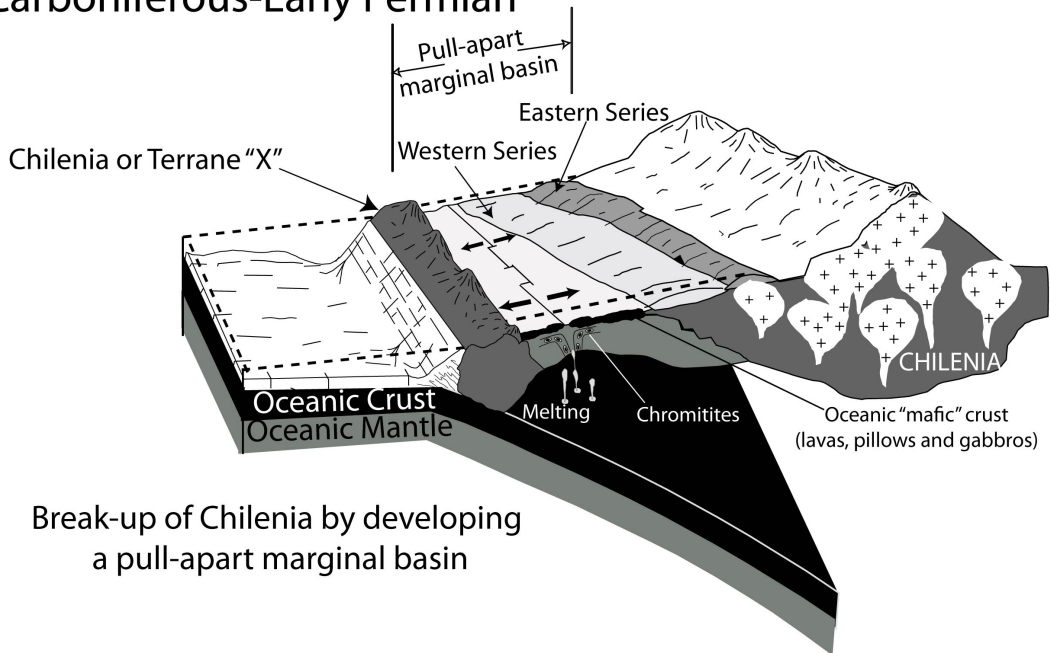


FIGURE 9.

Early Carboniferous

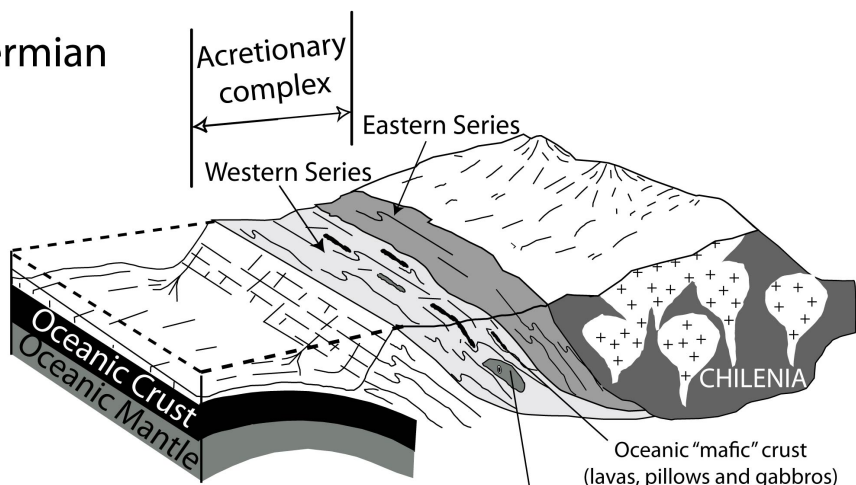


Carboniferous-Early Permian



Break-up of Chilenia by developing a pull-apart marginal basin

Late Permian



Metamorphism of peridotite ca. 286 Ma

Upper mantle rocks (peridotites and chromitites)

Table 1. Selected representative analyses of unaltered chromite at Centinela Bajo.

	011- P2-1	011- P2-9	5BF- f1-1	5BF- f1-2	5BF- f1-4	5BF- f1-5	5BF- f1-11	5BF- f1-12	5BF- f1-13	5BF- f2-31
TiO₂	0.23	0.23	0.14	0.13	0.13	0.12	0.13	0.14	0.12	0.13
Al₂O₃	17.96	18.52	17.69	17.71	17.70	17.71	17.65	17.87	18.50	17.78
V₂O₃	0.24	0.29	0.21	0.21	0.26	0.20	0.18	0.23	0.28	0.18
Cr₂O₃	50.80	48.71	51.55	51.42	51.21	51.81	51.46	51.07	51.58	51.41
Fe₂O₃	2.13	2.56	2.39	2.38	2.57	2.60	2.32	2.24	1.59	1.91
MgO	13.54	12.09	12.79	12.66	12.82	13.34	12.64	12.78	13.80	12.42
MnO	0.32	0.48	0.39	0.41	0.36	0.40	0.37	0.41	0.41	0.36
FeO	13.65	15.66	14.98	15.12	14.90	14.16	15.12	14.88	13.54	15.43
NiO	0.17	0.14	0.16	0.10	0.21	0.05	0.17	0.13	0.08	0.09
Total	99.03	98.68	100.32	100.14	100.15	100.38	100.02	99.74	99.90	99.71
Ti	0.01	0.01	0.00	0.00	0.00	0.00	0.00	0.00	0.00	0.00
Cr	1.26	1.22	1.28	1.28	1.27	1.28	1.28	1.27	1.27	1.28
Al	0.67	0.69	0.65	0.66	0.65	0.65	0.65	0.66	0.68	0.66
V	0.00	0.00	0.00	0.00	0.00	0.00	0.00	0.00	0.00	0.00
Fe³⁺	0.05	0.06	0.06	0.06	0.06	0.06	0.05	0.05	0.04	0.05
Mg	0.64	0.57	0.60	0.59	0.60	0.62	0.59	0.60	0.64	0.58
Mn	0.01	0.01	0.01	0.01	0.01	0.01	0.01	0.01	0.01	0.01
Fe²⁺	0.36	0.42	0.39	0.40	0.39	0.37	0.40	0.39	0.35	0.41
Ni	0.00	0.00	0.00	0.00	0.01	0.00	0.00	0.00	0.00	0.00
Zn	0.00	0.00	0.00	0.00	0.00	0.00	0.00	0.00	0.00	0.00
Cr#	0.65	0.64	0.66	0.66	0.66	0.66	0.66	0.66	0.65	0.66
Mg#	0.64	0.58	0.60	0.60	0.61	0.63	0.60	0.60	0.64	0.59
Fe³⁺#	0.12	0.13	0.13	0.12	0.13	0.14	0.12	0.12	0.10	0.10

Table 2. Platinum-group elements of chromitite samples from La Cabaña (in ppb).

	Centinela Bajo			Lavaderos		
	PODOB	CAB-7	CAB-7B	LA-C1	LA-C2	LA-C3
Os	22	29	43	27	20	34
Ir	157	93.3	153	60.5	74.1	66
Ru	126	136	92	79	108	106
Rh	12.9	7	9.8	6.9	8.8	8.5
Pt	28	19	12	< 5	13	6
Pd	< 2	10	9	< 2	12	3

* Detection limits are 5 ppb for Ru and Pt, 2 ppb for Os and Pd, 0.2 ppb for Rh and 0.1 ppb for Ir.

Table 3. Re, Os concentration (in ppb) and Os isotopic data of selected chromite samples from the La Cabaña ultramafic bodies

	Re	Os	$^{187}\text{Os}/^{188}\text{Os}$	$^{187}\text{Re}/^{188}\text{Os}$	$^{187}\text{Os}/^{188}\text{O}_i$	γ_{Os}	T_{MA}	T_{RD}
CEN-07	2.230	128.0	0.12522	0.08	0.12482	-0.93	505	466
CEN-08	0.3514	202.4	0.12710	0.008	0.12706	0.85	146	149
CEN-09	0.2049	78.69	0.12703	0.01	0.12698	0.78	156	160
LAC-1008	0.3225	37.66,	0.12675	0.04	0.12655	0.44	213	221

* $^{187}\text{Os}/^{188}\text{Os}$ initial γ_{Os} , T_{MA} and T_{RD} and model ages were calculated by comparison with the Os-isotope evolution of the enstatite Chondrite (present-day ECR $^{187}\text{Os}/^{188}\text{Os} = 0.1281 \pm 0.0004$, $^{187}\text{Re}/^{188}\text{Os} = 0.421$; Walker et al., 2002a) using the parameter λ for $^{187}\text{Re} = 1.555 \times 10^{-11} \text{ a}^{-1}$ from Shirey and Walker (1998). Note that T_{MA} and T_{RD} model ages are expressed in Ma.